CellPress
REVIEWS

Feature Review

Electric Phenomenon: A Disregarded Tool in Tissue Engineering and Regenerative Medicine

Lucília P. da Silva,[1,2] Subhas C. Kundu,[1,2] Rui L. Reis,[1,2,3] and Vitor M. Correlo[1,2,3,*]

Tissue engineering and regenerative medicine (TERM) are paving the way to the generation of functional and mature biological tissues that closely emulate cellular, biochemical, and mechanical cues. Electrical fields in the human body modulate myriad biological processes, such as synapses, muscle contraction, hearing, and wound healing, which were disregarded in TERM until recently. To preserve and improve tissue electrophysiology, cells can be loaded in electroactive biomaterials and stimulated with exogenous electrical fields. Here, we review how electrical stimulation and electroactive biomaterials can be used to instruct cells to create more mature and functional tissue-engineered constructs. We also highlight the most recent electroactive engineered tissues developed for TERM.

Importance of Electrical Fields in Tissue Engineering and Regenerative Medicine

Tissue and organ transplantations are major successes in healthcare technology because they can save the life of patients with terminal organ or tissue failure. However, these medical procedures are limited by tissue and/or organ availability and donor suitability. They are not accessible for all patients and are associated with prolonged waiting times, which threatens the life of patients. The field of tissue engineering and regenerative medicine (TERM) has emerged to respond to the lack of tissue and/or organ availability [3]. Engineered tissues are created through the combination of biomaterials, cells, and bioactive factors accurately selected to mimic the designated tissue. Bioengineered skin [4], trachea [5], blood vessels [6], bladder [7], and urethra [8] have already been successfully transplanted in humans, highlighting the viability of TERM strategies to replace and regenerate tissues and/or organs. However, recreating functional biological tissues and/or organs is challenging due to difficulties in recreating *in vitro* and *in vivo* environments that drive different cells to engineer a tissue.

Biological tissues are electrical systems with **electrical fields** (see Glossary) and currents due to the flow of charged ions and consequent formation of ion gradients (Box 1). These electrical fields mediate the communication of electrically excitable cells, such as neurons, and cardiac and skeletal muscle cells, which mediate important physiological processes, such as synapses, and cardiac and skeletal muscle contractions. The electrical currents existing in the body or created after injury are also responsible for myriad biological processes mediated by nonexcitable cells, such as the prohealing responses towards wound healing and regeneration [1]. Not only cells, but also extracellular matrix proteins, such as collagen, fibrin, and keratin, can generate electrical currents upon mechanical stress, a phenomenon known as **piezoelectricity** [2]. Given the significance of electrical fields in tissues and in their regeneration, bioengineered tissues are being developed with electrical cues to preserve cell–cell communication and to trigger tissue function.

The conductivities of biomaterials used in TERM strategies can be tailored to the same level as biological tissues [9]. Metals and metalloids, graphene and its derivatives, and conductive or piezoelectric polymers are being used to develop electroactive biomaterials. Cellular behavior is altered in the presence of electroactive biomaterials, especially after application of exogenous electric fields. This highlights the significance of electrical stimulation in TERM. Here, we review the effects of electrical fields and electroactive biomaterials on cell behavior, emphasizing the major progresses attained over the past 3 years for TERM applications. The types of electrical field that positively affect cell behavior are highlighted. Finally, we discuss the main features, advantages, and weaknesses of electroactive biomaterials, as well as the significance of electroactive biomaterials and electrical fields for TERM.

Highlights

The human body contains endogenous electrical currents due to the flow of ions. Electrical fields generated across cell membranes are involved in cell migration, proliferation, and differentiation, and the repair and regeneration of tissues.

Electroactive biomaterials incorporating metals, metalloids, graphene and graphene derivatives, conductive polymers, and piezoelectric polymers have low resistivity. Cell behaviors, such as attachment, migration, proliferation, and differentiation, are enhanced in electroactive biomaterials.

The synchronous contractibility of skeletal muscle and cardiac excitable cells can be modulated by applying external electrical fields.

Stem cells can be differentiated towards cardiac, skeletal muscle, neurogenic, or osteogenic lineages by applying specific external electrical fields even without the use of differentiation cell culture media.

[1]3Bs Research Group, I3B's – Research Institute on Biomaterials, Biodegradables and Biomimetics, Headquarters of the European Institute of Excellence on Tissue Engineering and Regenerative Medicine, University of Minho, AvePark 4805-017 Barco, Guimarães, Portugal

[2]ICVS/3Bs – PT Government Associate Laboratory, Braga/Guimarães, Portugal

[3]The Discoveries Centre for Regenerative and Precision Medicine, Headquarters at University of

*Corresponding author: vitorcorrelo@i3bs.uminho.pt

 https://doi.org/10.1016/j.tibtech.2019.07.002

Endogenous and Exogenous Electrical Fields

Biological tissues are electrical potencies with endogenous electrical currents due to the flowing of charged ions through ion pumps, gap junctions, or simple leaking across individual cells [10]. The difference in ion concentration inside and outside the cells generates an electric field across cell membranes, named the **membrane potential** (Box 1). Cells are commonly at a resting state, but alteration of the ionic balance and membrane potential may lead to the activation voltage-gated ion channels at cellular membranes. This alters the conformation of cellular membrane proteins, and the motion and concentration of molecules both at cell membranes and intracellularly [10]. The excited cells are able to form **action potentials** in response to small alterations of membrane potential that are critical for neural communication and for the contraction of the skeletal and cardiac muscle cells (Box 1) [11]. Nonexcitable cells are also able to respond to alterations of membrane potential with proliferation, orientation, migration, differentiation, and apoptosis that are involved *per se* in biological processes, such as the establishment of the left–right body asymmetry, the circadian rhythm, biological sensing, hearing, cell volume, secretion, contractility, cancer progression, wound healing, and regeneration [10,11].

The awareness of the **bioelectricity** in human tissues places exogenous electrical fields in the spotlight of research. Application of electrical fields *in vitro* (Box 2) is being explored not only to understand better the effect of endogenous electrical fields over cells, but also as a way to modulate cellular responses towards finding new treatments.

Endogenous electrical fields occurring in cortical neuronal networks are responsible for the synaptic plasticity and synchronization that are involved in the long-term consolidation of information [12]. Neuronal networks present several oscillatory bands covering frequencies from 0.05 Hz to 500 Hz, whereas a field strength on the order of mV is able to trigger membrane polarization and the generation of action potentials (Box 1) [12]. The application of exogenous electrical currents using physiological moderate frequencies (sinusoidal wave, 20 Hz, 0.02–0.04 V/cm) not only depolarizes, but also modulates neurons electrophysiology [13]. Exogenous electrical stimuli using low and almost subthreshold frequencies (<1 Hz) also evoke spike formation and network maturation in cortical neuron cultures [14], as well as in induced pluripotent stem cell (iPSC)- [15] and embryonic stem cell (ESC)- [16] derived neuron cultures. Exogenous electrical stimuli using suprathreshold frequencies may disguise endogenous electrical fields, which can be of interest for therapeutic purposes. This is corroborated by the suppression of cholinergic accumbens interneurons in acute rat brain slices after high-frequency electrical stimulation (100 μs, 140 Hz, 65 μA) [17]. Although explored at a lower extent, the use of low-voltage direct currents (0.05–1 V/cm) also promotes neuron migration [18] and outgrowth [19].

The contraction, synchrony, and rate of the myocardium are modulated by endogenous electrical fields. Exogenous electrical stimuli emulating endogenous electrical fields [alternating current (AC), 1–10 Hz, 2–5 ms, 1–5 V/cm] are applied to recreate the contraction of cardiomyocytes *in vitro* and further promote their maturation [20]. Notably, this chronic low-frequency electrical stimulus also improves the maturation of cardiomyocytes derived from human ESCs [21], iPSCs [22], and cardiac progenitor cells [23].

The contraction of the skeletal muscle is mediated through an excitation–contraction coupling process and is also modulated by endogenous electrical fields. The maturation and contraction of skeletal muscle myocytes are detected using physiological skeletal muscle rates (AC, 1 Hz, 2 ms, 40 V) [24]. Interestingly, the application of high-frequency electrical fields that emulate high load endurance exercise (AC, 100 Hz, 200 ms, 30 V) is able to trigger an increase in the levels of deoxyglucose uptake and lactate production, in contrast to chronic low-frequency electrostimulation [25].

Bone piezoelectricity is responsible for the endogenous electrical fields in bone [26]. Direct currents proportional to bone mechanical loading can be generated in the bone; for example, direct currents on the order of 300 mV are generated in the tibia in humans with walking [26]. Both high-voltage (10–15 V/cm) and low-voltage (<5 V/cm) exogenous direct currents are capable of triggering human

Glossary

Action potential: alteration of the membrane potential (membrane depolarization followed by repolarization) of excitable cells owed to the opening of voltage-gated ion channels.
Bioelectricity: electric fields in the human body that modulate the behavior of cells and tissues.
Electric field: difference of electric potential between two points.
Electrical conductivity (σ): ability of a biomaterial to conduct electrical current; is inversely proportional to the resistivity.
Electrical impedance (Z): total opposition to the motion of electrons in response to an alternating current. Impendence comprises a real part: the resistance (R): and an imaginary part: the reactance (X).
Electrical reactance (X): inertia against the motion of electrons due to inductance (L) and capacitance (C).
Electrical resistance (R): friction against the motion of electrons in response to a direct current (DC).
Electrical resistivity (ρ): resistance of a biomaterial to conduct electricity.
Inductance (L)/Capacitance (C): ability of a biomaterial to store energy in the form of a magnetic and/or electric field.
Membrane potential: electric fields existing across cell membranes owing to the difference in ion concentration inside and outside the cell.
Piezoelectricity: electric current that accumulates in materials upon application of mechanical stress.

Box 1. Action Potentials

An electric field (mV/mm) is the difference in electric potential between two points. The difference in ion concentration inside and outside the cell generates an electric field across the cell membrane, named the 'membrane potential'. Cells have a resting membrane potential of different magnitudes: nonexcitable cells present a higher membrane potential (~–40 mV), whereas excitable cells present a lower membrane potential (~–90 mV), reacting quickly to small ion changes [11]. Excitable cells are capable of generating action potentials (Figure IA). Opening of voltage-gated sodium or calcium channels in cell membranes leads to an influx of cations into the cells, causing membrane depolarization and action potentials (Figure I). Opening of voltage-gated potassium channels leads to the efflux of potassium out of the cells, causing membrane repolarization to the resting potential (Figure I). A small period of membrane hyperpolarization occurs due to the delayed closure of potassium channels (Figure I) [143].

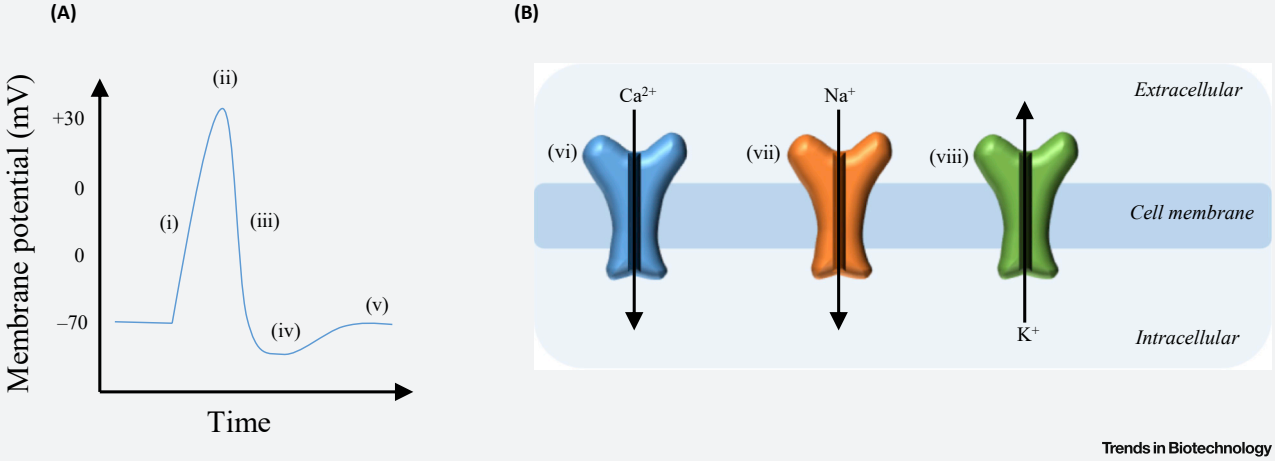

Figure I. Electrical Properties of Cell Membranes and Ion Channels.

(A) Graphical representation of membrane potential; (B) Schematic representation of ion flux through voltage-gated channels. (i) membrane depolarization; (ii) action potential; (iii) membrane repolarization; (iv) membrane hyperpolarization; (v) resting potential; (vi) voltage-gated calcium channel; (vii) voltage-gated sodium channel; and (viii) voltage-gated potassium channel.

SaOS-2 cell elongation perpendicularly to the electrical field [27]. Migration towards the anode and increase in intracellular calcium can also be observed, although at a higher extent with strong electrical fields [27]. Moreover, application of alternating currents with mild to high frequencies (10 Hz–60 kHz) can successfully promote the differentiation of osteoblast cells [28]. The osteogenic (but not adipogenic or chondrogenic) differentiation of human bone marrow-derived mesenchymal stem cells (hBMSCs) is also evident even in the absence of a osteogenic cell culture medium [29].

Considering that exogenous electrical fields are affected by the tissue environment (i.e., electrical resistivity and electrical impedance of tissues, concentration of ions within the highly hydrated extracellular matrices), different electrostimulation protocols [acute (min) to chronic (days), short (2–5 ms) to long (10–100 ms), low (1–100 mV/cm) to high (1–2 V/cm) voltages, and low (1–10 Hz) to high (10–100 Hz) frequencies] are being used to study the effect of endogenous electrical fields and to foster the discovery of new treatments. In fact, electrical stimulation is the basis of some clinical treatments intended to activate the healing of injured tissues, for instance to treat anxiety, depression, insomnia [30], and fractured bones [26]. Further advances will be achieved by improving the current knowledge on endogenous electrical fields, standardization of effective electrostimulation protocols, and the development of electroactive biomaterials that preserve the electrophysiology of the cells and potentiate the electrostimulation of cells.

Electroactive Biomaterials for TERM

The electrical properties of biological tissues are determined by the diffusion of charged ions within the highly hydrated extracellular matrices. Recreation of this electric environment in bioengineered

Box 2. Tools for Cell Electrostimulation

An *in vitro* electrical stimulation set-up requires three main components: (i) a petri dish or well-plate containing cells bathed in an electrolyte medium and/or solution; (ii) an electrical power supply; and (iii) conductive electrodes to connect the electrical power through the electrolyte solution in which the cells are cultured (Figure I).

Different methods are used to apply electrical stimulation *in vitro*, including direct stimulation (Figure I), inductive stimulation, capacitive stimulation, and combined stimulation [144]. Although direct stimulation presents some disadvantages (e.g., formation of a capacitive bilayer; toxicity of electrodes commonly made of platinum, titanium, stainless steel, gold, graphene or carbon; pH alteration; and faradaic byproducts from electrolysis) in relation to the other methods, it is widely selected by researchers possibly due to the simplicity of its use [144]. There is a range of parameters that can be varied in electrical stimulation. The electrical stimuli can be induced using a direct (DC) or alternating current (AC) (Figure I). The level of the current (A), the amplitude of the voltage (V), and the duration of the electrical stimuli (continuous or cyclic, from hours to days) can be varied in DC electrical stimuli. In AC electrical stimuli, the type of wave (monophasic or biphasic; sine, square, triangular, and others), the duration of the electrical stimuli (continuous or cyclic, from hours to days), the frequency (Hz), and the pulse width (sec) can be altered.

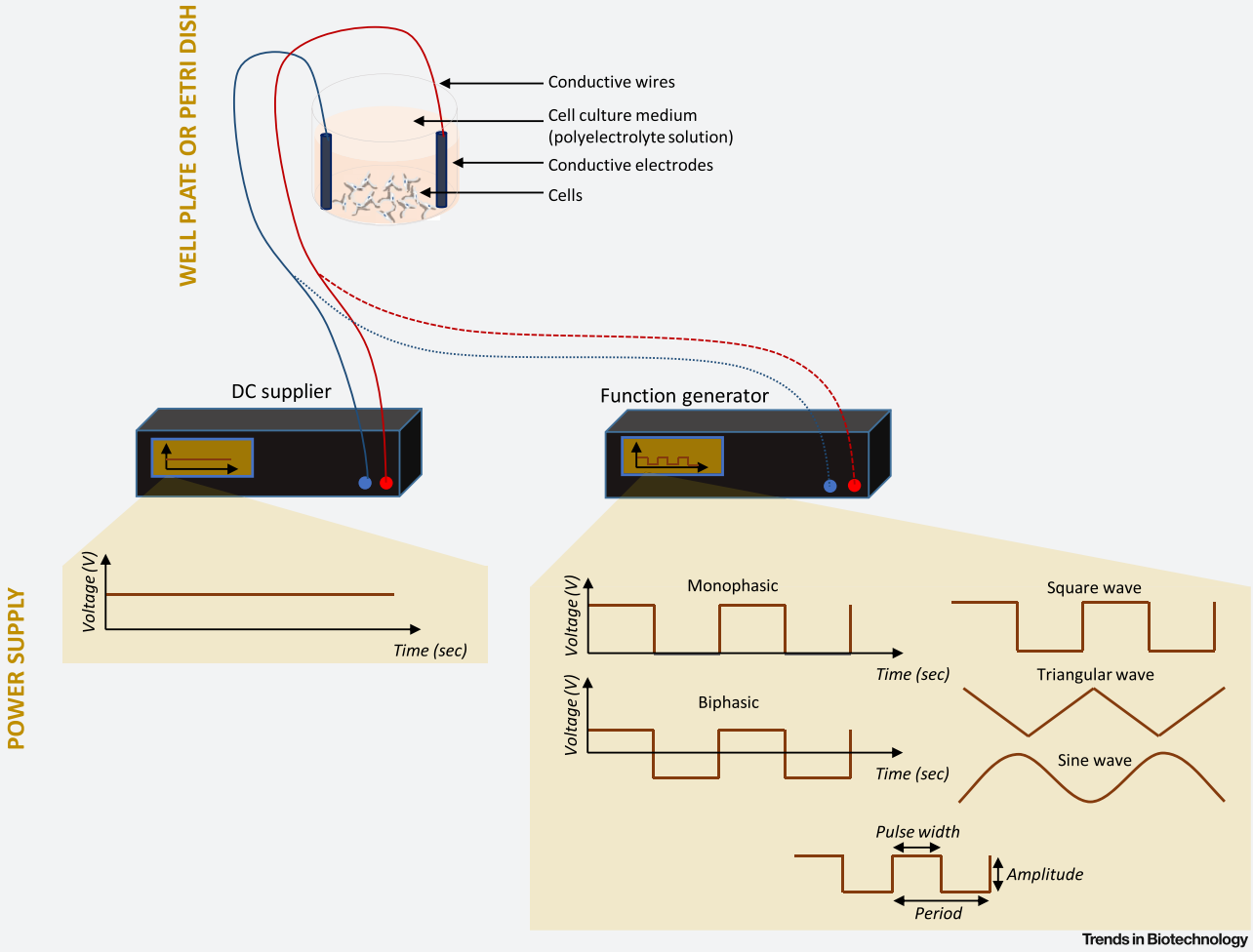

Figure I. Electrostimulation Apparatus for *In Vitro* Cell Culture.

Abbreviation: DC, direct current.

tissues is challenging because most of the biomaterials used in TERM present high levels of electrical resistivity, limiting the flow of ions. Most of the biomaterials used in TERM (scaffolds, hydrogels, electrospun meshes, membranes, and micro- and nanoparticles) are based on polymers of synthetic [e.g.,

polyethylene glycol (PEG), poly(lactic-co-glycolic acid) (PLGA), polycapralactone (PCL), and polyurethane (PU)] or natural [e.g., collagen (COL), silk fibroin (SF), alginate, chitosan (CHT), hyaluronic acid (HA), and gellan gum (GG)] origins. They are not electrical conductors *per se*. To recreate the semiconducting properties of biological tissues ($\sigma = \sim 10^0$ S/m) [9], bioengineers are exploring electroactive biomaterials with higher **electrical conductivity** (lower electrical resistivity) and lower electrical impedance values that make them capable of generating electrical currents (Figure 1, Box 3). Here, we describe the most recent electroactive biomaterials developed for TERM, emphasizing not only their electrical features, but also other properties that are essential for TERM applications.

Metals and Metalloids

Metals are high conductors of electrical charge ($\sigma = 10^5$–10^7 S/m) due to the presence of valence electrons in their outer shell that can move freely to conduct electricity. Titanium alloys are used in TERM due to their high mechanical strength, corrosion resistance, bioinert properties, and high conductive

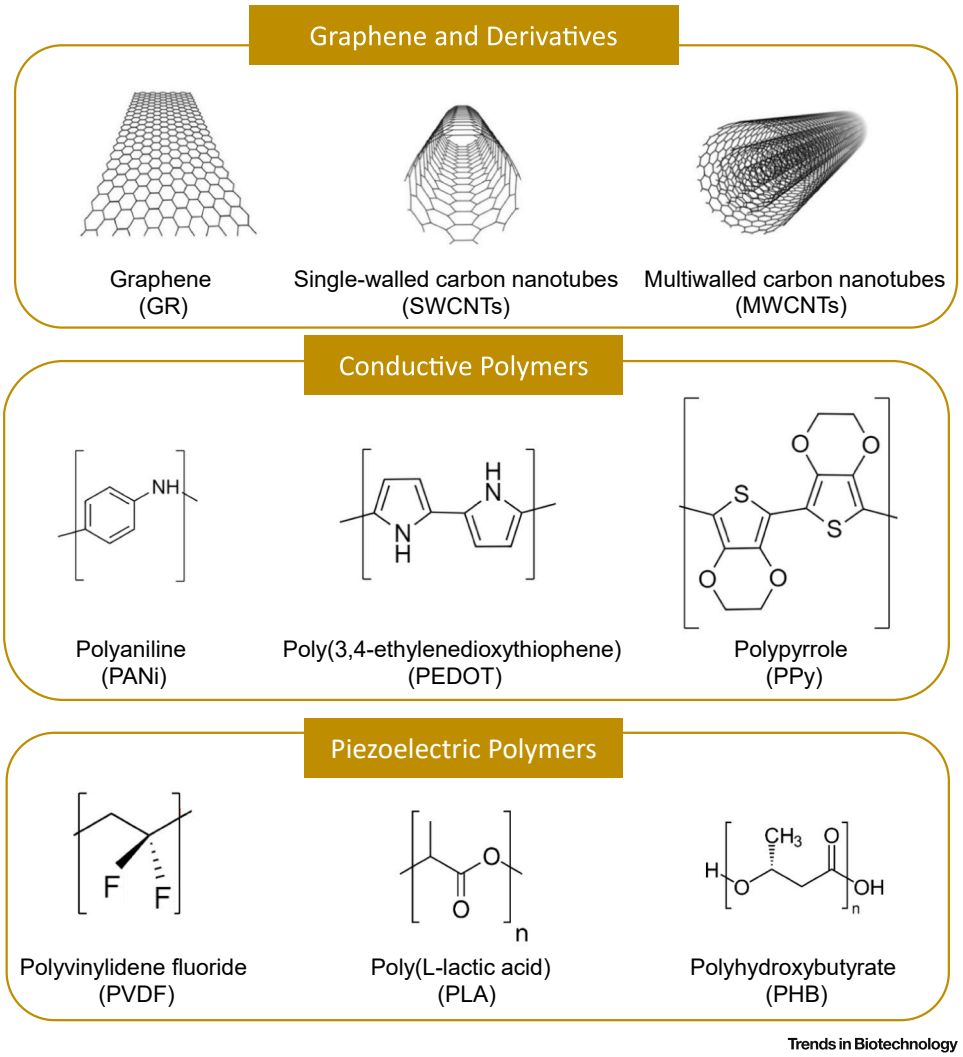

Figure 1. Electroactive Biomaterials Used for Tissue Engineering and Regenerative Medicine (TERM). Graphene and its derivatives, and conductive and piezoelectric polymers contain free valence electrons that give them electroconductive features. Adapted, with permission, from [146].

values. The electrical properties of titanium alloys, including titanium surfaces/coatings, titania nanotubes (TiO_2 or TNTs) [31] and barium titanate ($BaTiO_3$) [32,33] are being explored to improve cellular responses (Table 1). The piezoelectric nature of barium titanate (d_{33} = ~5–8 pC/N) is particularly useful for improving cell performance upon application of mechanical loads [32,33]. Gold nanorods (AuNRs) are used for many biomedical applications, including sensing, imaging, theranostics, and phototherapy owing to their structural, optical, electronic, magnetic, and catalytic properties [34]. Gold is another metal with high mechanical strength and corrosion resistance that is being explored TERM (Table 2). Their electrical properties have been exploited to reduce the impedance values of biomaterials, particularly in gelatin methacrylate (GelMA)-based hydrogels [35] and bioinks [36], and to improve the photoconductivity of silk protein hydrogels [37]. The conductivity of metalloids,

Box 3. Tools to Determine the Electrical Properties of Biomaterials

The electrical resistivity of a uniform biomaterial can be measured using a two- or four-probe station linked to an ammeter and/or voltage source. A DC with a predefined voltage (s) is applied to the biomaterial and the current passing through the biomaterial is measured. The **electrical resistance**, resistivity, and conductivity of electroactive biomaterials can be calculated using Equations I–III and analyzed using a current-voltage plot (Figure IA).

$$R = \frac{U}{I} \quad [I]$$

$$\rho = R\frac{A}{l} \quad [II]$$

$$\sigma = \frac{1}{\rho} \quad [III]$$

where σ is the conductivity (S/m); ρ is the resistivity (Ω·m); I is the current (A); U is the voltage (V); R is the resistance (Ω); L is the length of the material (m); and A is the cross-sectional area of the material (m^2).

The electrical impedance of a biomaterial can be measured using an electrochemical impedance spectroscope (EIS) or a potentiostat, galvanostat, or sine wave generator with three electrodes, including the reference electrode (Ag/AgCl), a counter electrode (Pt), and a working electrode (electroactive biomaterial). An AC with a predefined amplitude (voltage) is delivered to an electrolyte solution (physiological solution: 0.1 M NaCl) at a frequency range and the current is measured. The impedance, reactance (inductive and capacitive), and resistance of electroactive biomaterials can be calculated using Equations IV–IX and analyzed in the bode (Figure IB) or Nyquist (Figure IC) plots.

$$Z\omega = U\omega / I\omega \quad [IV]$$

$$Z = R + jX \quad [V]$$

$$|Z| = R^2 + X^2 \quad [VI]$$

$$X = X_L + X_C \quad [VII]$$

$$X_L = 2\pi\omega L \quad [VIII]$$

$$X_C = -\frac{1}{2\pi\omega C} \quad [IX]$$

where Z is the impedance (Ω); U is the **potential** (V); I is the current (A); ω is the frequency (Hz); R is the resistance (Ω); j is the square root of –1; X is the **reactance** (Ω); X_L is the inductive reactance (Ω); X_C is the capacitive reactance (Ω); L is the **inductance** (H); and C is the **capacitance** (F).

Cyclic voltammetry (CV) provides information relative to the redox reactions of a biomaterial [145]. Redox reactions can be analyzed using a potentiostat and/or galvanostat with three electrodes, including the reference electrode (Ag/AgCl), a counter electrode (Pt), and a working electrode (electroactive biomaterial). An AC with a predefined cyclic potential (voltage) is delivered to an electrolyte solution (physiological solution: 0.1 M NaCl) at a predefined frequency and the current resultant from the flow of electrons between the working and counter electrode is measured. The charge storage capacity (CSC) of the electroactive biomaterials can be calculated by analyzing the current-potential plot (Figure ID) through the integration of the area enclosed by the voltammogram.

Piezoelectricity can be analyzed using an electrochemical impedance spectroscope (EIS), laser doppler vibrometer (LDV) or piezoresponse force microscopy (PFM). An electric current is applied to the biomaterials and the piezoelectric coefficient (d) is measured. The piezoelectric coefficient (d) provides information relative to the degree of orientation of the electric domain of biomaterials into the external electric field and can be calculated using Equation X and analyzed from the resulting plots (Figure IE,F).

$$d = \frac{P}{\sigma}, \quad [X]$$

where d is the piezoelectric coefficient (pC/N); P is the polarization; and σ is the stress.

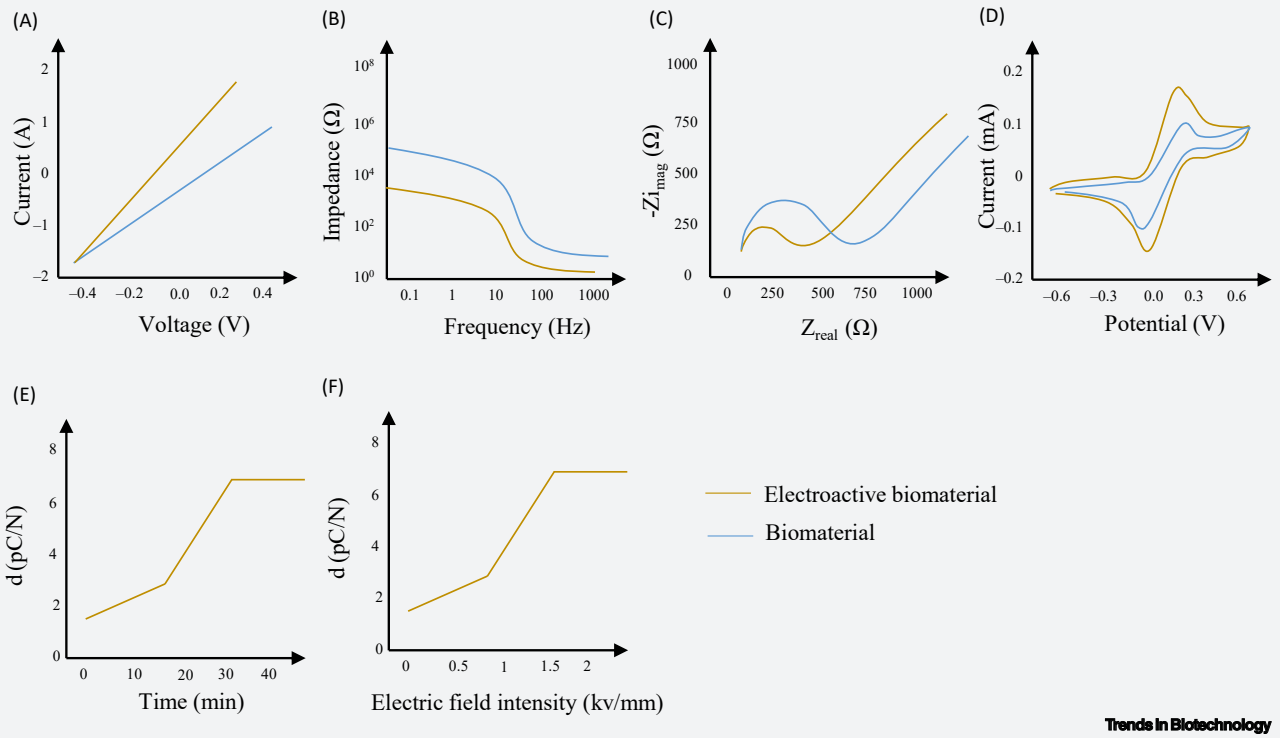

Figure I. Graphical Representations of the Electrical Properties of (Electroactive) Biomaterials.

(A) Current-voltage plot obtained by resistivity measurements; (B) Bode and (C) Nyquist plots obtained by impedance measurements; (D) current-potential plot obtained by cyclic voltammetry; (E) piezoelectric modulus-time; and (F) piezoelectric modulus-electric field intensity plots obtained by piezoelectric measurements.

although at lower levels (semiconductors, $10^{-6}<\sigma>10^{4}$ S/m), have also been investigated for TERM applications (Table 2). Inspired by their extensive applications in electronics to prepare integrated circuits, silicon nanowires (SiNWs) have been integrated into cellular spheroids to improve the electrical environment [38].

Although metals/metalloids have useful mechanical and conductivity properties, their use has diminished over the past few years due to their lack of integration with the host tissue and biocompatibility issues. Despite *in vitro* data showing the corrosion-resistant properties of metal/metalloids, after years of electrochemical attack *in vivo*, metals/metalloids start leaching nonbiodegradable toxic metal ions into the body fluid [39]. Several cases of infection have been reported in patients after implantation of these metals due to bacteria adhesion to the surfaces of metal/metalloid implants and the consequent development of biofilms [40]. Such adverse effects lead to significant clinical failure. Different techniques are used to overcome these drawbacks by modifying the metal/metalloid surfaces through the deposition of suitable coatings, development of a passivation-oxide layer, ion-beam surface modification, and surface texturing [39]. However, the functionality of these strategies remains to be confirmed.

Graphene and Its Derivatives

Graphene (GR) is a carbon allotrope that comprises carbon atoms arranged in a hexagonal lattice forming a 2D sheet (Figure 1). Rolling of graphene sheet(s) results in 3D tubular structures named

Table 1. Cell Responses to Electroactive Biomaterials and Electrical Fields in Bone Tissue Engineering[a]

Electroactive biomaterials					
Electroactive biomaterial	**Other biomaterials**	**Electrical features**	**Cell type**	**Cellular response**	**Refs**
$BaTiO_3$; 80–100%	HAp	d_{33} = 1.3–6.8 pC/N	OBs	↑ Cell growth, viability and ALP activity (with mechanical loading), dependent on [BaTiO3] (relative to pristine)	[32]
GO; 3%	PTMC	$\sigma = 10^{-1}$ S/m	hASCs	↑ Cell attachment and proliferation (relative to pristine)	[130]
f-CNTs; 0.01–1%	SF	–	MG-63 h-MSC	↑ Mineralization, ALP activity, expression of osteogenic genes (*COL1*, *RUNX2*, *ALP*, *BSP*, *OCN*, *OPN*), dependent on [CNTs] (relative to pristine)	[147]
PANi; 0.8–2.4 mM	PLA	$\sigma = 10^{0}$ S/m	rbBMSCs-OBs	↑ Metabolic activity, expression of osteogenic genes (*ALP*, *Ocn*, *Runx2*) and calcium mineralization, dependent on PANi amount (relative to pristine)	[52]
PEDOT; 1.25%	–	$\sigma = 10^{-2}$ S/m	MC3T3-E1	Expression of osteogenic genes (*ALPL*, *COL1A1*, *RUNX2*) and proteins (Ocn), calcium mineralization (relative to pristine)	[74]
PVDF-Ti	–	d33 = –28 pC/N	BMSCs	↑ Cell proliferation, ↑ ALP activity, ↑ expression of osteogenic genes (*ALP*, *COLI*, *OP*) (relative to nonpolarized PVDF)	[81]
β-PVDF	–	–	hBMSCs hBMSC-OBs	↓ MSC pluripotency markers (CD90, CD105, CD73), ↑ ALP activity (hBMSCs, relative to glass), ↑ expression of osteogenic protein (Ocn), ↓ Ca^{2+} mineralization (hBMSC-OBs, relative to glass)	[84]
PVDF-TrFe and $BaTiO_3$	–	–	rBMSCs-OBs rASCs-OBs	Osteogenic differentiation observed through expression of osteogenic genes (*Runx2*, *ALP*, *BSP*, *Ocn*), ALP activity and Ca^{2+} mineralization	[33]
PHB and PANi; 6% and 2%	PCL	–	hBMSCs-OBs	↑ Cell adhesion and proliferation (relative to pristine), osteogenic differentiation observed through presence of Ca^{2+} mineralization and ALP activity	[93]
Electrical fields					
DC					
Electrical field	**Electro-active biomaterials**	**Cell types**	**Cellular responses**		**Refs**
I = 0.01 mA Δt = 12 h/day for 14 days	PPy and Ti	MC3T3-E1	↑ ALP activity, ↑ β-GP and calcium deposition (relative to nonstimulated cells)		[131]
I = 0.2 mA Δt = 4 h	Ti, PPy, and PLGA	MG63	Earlier onset of osteogenesis and ↑ calcium levels with Ca:P ratios similar to those of natural bone (relative to nonstimulated cells)		[132]
I = 0.2 mA Δt = 4 h/day for 21 days	PPY and PCL	MC3T3-E1 hASCs	↑ Cell viability, ALP activity, and calcium deposition in both cells, ↑ expression of osteogenic proteins (Runx2, Ocn, Opn) by MSCs (relative to nonstimulated cells)		[133]

(Continued on next page)

Table 1. ***Continued***

Electrical fields				
DC				
Electrical field	Electro-active biomaterials	Cell types	Cellular responses	Refs
I = 0.2 mA Δt = 4 h/day for 21 days	PPy and CHT	hASCs HUVECs	↑Calcium deposition and osteogenic differentiation with co-culture and electrical stimulation, ↑ CD31 expression of HUVECs (relative to nonstimulated cells), responses mediated by BMP-2 and VEGF	[134]
U = 0.01 V/cm Δt = 1 h/day for 3 weeks	ß-TCP	ASC-OBs	↑ Osteogenic differentiation, ↑ expression of osteogenic genes (*TGFb1*, *BMP2*, *Opn*, calmodulin) (relative to nonstimulated cells)	[135]
U = 0.2–0.4 V/cm Δt = 8 days	TiO_2	rMSCs rMSCs-OBs MC3T3-E1	↑ Osteogenic induction following downstream calcineurin/CAMKII/NFAT signaling, formation of plasma membrane protrusions and transport of Cx43 to these protrusions, ↑ intracellular calcium, ↑ calcium mineralization, ↑ expression of osteogenic proteins (Ocn, Osx, Cx43) (relative to nonstimulated cells)	[31]
U = 1.5 V Δt = 1.5 h/day for 7 days	MWCNTs and PLLA	rBMSCs-OBs	↑ Cell proliferation, ↑ cell elongation ↑ALP activity ↑ calcium and COLI, ↑ expression of osteogenic genes (*Runx2*, *BMP2*, ALP, *Opn*, *Ocn*, *COLI*) (relative to no-stimulated cells), stronger if ES applied at early stages	[136]
U = 2 V Δt = 4 h/2 days for 12 days	PPy	rBMSCs-OBs	↑ Expression of osteogenic markers (COLI and ALP) (relative to nonstimulated cells)	[137]
U = 15 V Δt = 10 min/day for 4 weeks	HAp-$CaTiO_3$	hMSCs	↑ Calcium mineralization, ↑ expression of osteogenic markers (ALP, COLIA, Runx2, Ocn) (relative to nonstimulated cells)	[138]
AC				
Electrical field	Electro-active biomaterials	Cell types	Cellular responses	Refs
Biphasic wave ω = 1 Hz Pulse width = 10 ms Δt = 2 days	PPy	MC3T3-E1	↑ ALP activity, ↑ expression of osteogenic genes (*ALP*, *COLI*, *Runx2*, *Ocn*) only with daily suitable electrical stimulation (relative to nonstimulated cells)	[139]
Biphasic wave I = 0.01 mA ω = 100 Hz Pulse width = 2.5 ms Δt = 4 h/day for 7 days	GO and PTMC	hASCs-OBs	↑ Expression of osteogenic markers (ALP and COLI) (relative to nonstimulated cells)	[130]
I = 0.5 mA ω = 0.004 Hz Δt = 20 min twice a week for 2 weeks	CNT, COL , silicone	hASCs-OBs	↑ Osteogenic differentiation, ↑ calcium mineralization (relative to nonstimulated cells)	[140]
Square wave U = 0.0036 V/cm ω = 0.001–100 Hz Pulse width = 7 ms Δt = 14 days	PPy	rBMSCs	↑ Calcium mineralization, ↑ expression of osteogenic genes (*BSP*, *COLI*, *ALP*, *RUNX2*, *Ocn*) dependent on both frequency and voltage (relative to nonstimulated cells)	[137]

(Continued on next page)

Table 1. ***Continued***

AC				
Electrical field	**Electro-active biomaterials**	**Cell types**	**Cellular responses**	**Refs**
U = 0.1–0.5 V ω = 1–5 Hz Pulse width = 1 μs Δt = 1–3 days	GR	hBMSCs	↑ Expression of early and mature osteogenic markers (RUNX2 and Opn) (relative to nonstimulated cells)	[102]
U = 0.1–0.5 V ω = 60 000 Hz Δt = 1 h/day for 28 days	SF	hBMSCs-OBs	↑ Expression of more mature osteogenic markers (BSP) and mineralization (relative to nonstimulated cells)	[141]
U = 2 V ω = 100 Hz Δt = 2 h/day for 14 days	ANi pentamer, CHT and HAp	hBMSCs	↑ Expression of osteogenic markers (Ocn, ALP, ON, Runx2) (relative to nonstimulated cells)	[142]

[a]Abbreviations: β-GP, β-glycerophosphate; β-PVDF, β-polyvinylidene fluoride; β-TGP, β-triglycerophosphate; ALP, alkaline phosphatase; ANi, aniline; ASCs, adipose-derived stem cells; ASC-OBs, adipose-derived mesenchymal stem cells primed towards osteoblast lineage; ATDC5, murine chondrogenic cell line; BG, bioactive glass; BMP2, bone morphogenetic protein 2; BMSC-OBs, bone marrow-derived stem cells primed towards osteogenic lineage; BSP, bone sialoprotein; Ca/P, calcium/phosphate; CNT, carbon nanotube; Cx43, connexin 43; DC, direct current; ECM, extracellular matrix; f-MWCNTs, functionalized multiwalled carbon nanotubes; GO, graphene oxide; GR, graphene; h, human; HAp, hydroxyapatite; hASCs, human adipose-derived stem cells; HUVECs, human umbilical vein endothelial cells; I, intensity; MC3T3-E1, murine pre-osteoblast cell line; MG-63, human osteosarcoma cell line; MSC-OBs, mesenchymal stem cells differentiated towards osteoblast lineage; MWCNTs, multiwalled carbon nanotubes; OBs, osteoblasts; Ocn, osteocalcin; ON, osteonectin; Opn, osteopontin; Osx, osterix; PANi, polyaniline; PEDOT, poly(3,4-ethylenedioxythiophene); PLA, polylactic acid; PPy, polypyrrole; PTFE, polytetra-fluoroethylene; PTMC, poly(trimethylene carbonate); PVDF, polyvinylidene fluoride-titanium; PVDF/TrFe, poly(vinylidenefluoride-co-trifluoroethylene); r, rat; rb, rabbit; Runx2, Runt-related transcription factor 2; SBF, simulated body fluid; TGF-β1, transforming growth factor β1;Si, silicon; U, voltage; VEGF, vascular endothelial growth factor; Δt, time variation; ω, frequency; ↑, upregulation; ↓ downregulation.

single-walled (SWCNTs) or multiwalled (MWCNTs) carbon nanotubes (CNTs) depending on the number of enrolled sheets (Figure 1). The presence of free electrons in GR and its derivatives result in high electrical properties ($\sigma = 10^6$–10^7 S/m) that, together with their mechanical strength, improve not only the conductivity of biomaterials to semiconductors [$\sigma = 10^{-5}$–10^2 S/m; $Z = 10^2$–10^5 Ω·m (at 1 Hz)], but also their mechanical properties (Tables 1–4).

GR and its derivatives also present critical limitations. The aromatic chemistry of GR makes it hydrophobic and insoluble in water-based solutions [41–43], making it prone to aggregate and more difficult to degrade [44–47]. In addition, GR degradation is already limited to particular types of microorganism and oxidase/peroxidase enzymes. The hydrophobic nature of GR is also associated with cytotoxicity because it easily interpenetrates the cellular hydrophobic membranes, leading to their disruption [48]. Impurities, high dimensions, surface defects, and protein adsorption are features that are also associated with GR toxicity [48]. To overcome these limitations, smaller amounts of GR and noncovalent (adsorption of molecules using coatings) and covalent (conjugation of carboxylate or hydroxyl groups) functionalization of GR are being used to improve their water solubility [49,50] and biocompatibility [46,47,51].

Conductive Polymers

Polymers with free valence electrons in their core that are not occupied by covalent bonding with neighboring atoms are conductive. Polyaniline (PANi), polypyrrole (PPy), and poly (3,4-ethylenedioxythiophene) (PEDOT) are examples of conductive polymers that are gaining notoriety in TERM (Tables 1–4, Figure 1). These polymers can be prepared by polymerizing their corresponding monomers [i.e., aniline (ANi), pyrrole (Py), and 3,4-ethylenedioxythiophene (EDOT)] through electrochemical polymerization, using a two-electrode workstation potentiostat at the surface of an electrode, or

Table 2. Cell Responses to Electroactive Biomaterials and Electrical Fields in Skeletal Muscle Tissue Engineering[a]

Electroactive biomaterials					
Electroactive biomaterial	**Other biomaterials**	**Electrical features**	**Cell type**	**Cellular response**	**Refs**
GR; 0.3–2%	PCL	$\sigma = 10^0$ S/m $Z = 10^3$ Ω·m	C2C12	↑ Cell differentiation, ↑ myotube fusion, ↑ expression of myogenic proteins (MHC) (relative to pristine)	[50]
rGO; 0.3%	PAAm	$Z = 10^2$ Ω·m	C2C12	↑ Cell proliferation, ↑ cell differentiation, ↑ myotube formation, expression of myogenic genes and/or proteins (MyoD, Myog, MHC) (relative to pristine)	[123]
rGO; 0.4–2%	PCE	$\sigma = 10^{-2}$ S/m	C2C12	↑ Cell proliferation, ↑ cell differentiation ↑ myotube fusion, ↑ expression of myogenic genes and/or proteins (MyoD, Myog, TnT, MHC) (relative to pristine)	[46]
GR and GO; 0.3–1.7%	PANi and PAN	$\sigma = 10^{-1}$ S/m	m-Sat	↑ Cell viability, ↑ cell differentiation, ↑ expression of myogenic genes and/or proteins (MyH, α-SA, MyoD, TnI, Pax7) and adhesion genes (*CD34*, M-cadherin) (relative to pristine)	[124]
PANi; 5%	PAN and GEL	$\sigma = 10^{-3}$ S/m	m-Sat	Cell viability, cell differentiation, expression of myogenic genes (*Myh2*, *MyoD*, *aSA*)	[71]
PANi; 5–10%	GEL	$\sigma = 10^{-1}$ S/m	C2C12	↑ Cell differentiation, ↑ myotube formation and maturation, ↑ expression of excitation-contraction genes *DHPR* (Cav1.1 and β1.1) and *RyR* (*RyR1* and *RyR3*) and colocalization (relative to pristine)	[72]
PANi; 1 M	GG	$\sigma = 10^{-2}$ S/m	C2C12	↑ Cell adhesion and spread, ↑ expression of myogenic proteins (MHC) (relative to pristine)	[58]
PASA; 1–2%	SF	$\sigma = 10^{-5}$ S/m	L929 C2C12	Cell adhesion and proliferation (L929, C2C12), ↑ expression of myogenic genes (*MyoD*, *Myog*, *TnT1*) (C2C12) (relative to pristine)	[59]
PPy; 0.1 M	GG	$\sigma = 10^{-4}$	L929 C2C12	↑ Cell adhesion and spread (relative to pristine)	[60]
PPy	PTMC	$Z = 10^3$ Ω·m	hASC-SMs	↑ Cell proliferation, ↑ expression of myogenic proteins (calponin, MHC) (relative to pristine)	[128]
PEDOT and MWCNT; 20%	–	–	C2C12	Cell differentiation, myotube fusion, cell alignment, expression of myogenic proteins (MHC) (relative to pristine)	[127]
β-PVDF	–	–	C2C12	↑ Cell differentiation, ↑ myotube fusion, ↑ myotube maturation index, ↑ myotube length, diameter, and number, ↑ cell alignment with oriented fibers, ↑ expression of myogenic protein (MHC) (relative to pristine)	[87]

Electrical fields				
AC				
Electrical field	**Electroactive biomaterial**	**Cell type**	**Cellular response**	**Refs**
U = 0.1 V/cm ω = 1 Hz Pulse width = 2 ms Δt = 7 days	COL and Matrigel	hSM cell line	Presence of sarcomeres, calcium oscillations, and expression of myogenic proteins (α-SA, myosin, RyR, SERCA2), synchronous contraction (relative to nonstimulated cells)	[125]

(Continued on next page)

Table 2. *Continued*

Electrical fields				
AC				
Electrical field	Electroactive biomaterial	Cell type	Cellular response	Refs
U = 5 V ω = 1 Hz Pulse width = 10 ms Δt = 4 h/day for 3–7 days	rGO and PAAM	C2C12	↑ Expression of myogenic genes (*MyoD*, *Myog*, *MHC*) but ↓ expression of *Pax7* (relative to nonstimulated cells)	[123]
Square wave U = 6 V ω = 1 Hz Pulse width = 1 ms Δt = 1 day	PANi and GEL	C2C12	Calcium transients and myotube contraction.	[72]
Biphasic square wave U = 20 V ω = 1–10 Hz Pulse width = 50 ms Δt = 10 days	Thrombin, Matrigel, and fibrinogen	C2C12	Ability to generate up to 1.7 mn (3.2 kPa) of passive tension force and 300 mn (0.56 kPa) of active tension force (relative to nonstimulated cells)	[126]
Sine wave U = 60–80 V Pulse width = 10 ms ω = 0.5–8 Hz	MWCNT and PEDOT	C2C12	Contraction modulated by frequency of electric fields, formation of flexible movement with electrical stimulation, faster relaxation kinetics of TE construct (relative to nonstimulated cells)	[127]

[a]Abbreviations: β-PVDF, β-polyvinylidene fluoride; ASC-SMs, adipose-derived mesenchymal stem cells primed to smooth muscle cell lineage; C2C12, mouse myoblast cell line; CSA, camphorsulfonic acid; DHPR, dihydropyridine receptor; GEL, gelatin; GO, graphene oxide; GR, graphene; h, human; m, murine; MHC, major histocompatibility complex; MWCNTs, multiwalled carbon nanotubes; MYH, myosin heavy chain; Myog, myogenin; PAN, polyacrylonitrile; PANi, polyaniline; PASA, PANi-co-N-(4-sulfophenyl) aniline); Pax 7, paired box 7; PCE, poly[citric acid-octanediol-poly(ethylene glycol)]; PEDOT, poly(3,4-ethylenedioxythiophene); PPAM, polyacrylamide; PPy, polypyrrole; PTMC, poly(trimethylene carbonate); rGO, reduced graphene oxide; RyR, ryanodine receptor; Sat, satellite cells; SERCA, sarco/endoplasmic reticulum Ca2+-ATPase; SM, skeletal myocyte; T, tissue engineering; TnI, troponin I; TnT, troponin T; Tnt1, troponin T1; U, voltage; ↑ α-SA, α-sarcomeric actinin; ω, frequency; Δt, time variation; ↑, upregulation; ↓ downregulation.

through oxidation. Ammonium persulfate (APS) in HCl [52–64], ferric chloride [65,66], and hypophosphorous acid [67] are common oxidants used for monomer polymerization. During or after the synthesis, dopants (with counter ions) are added to stabilize the conductive polymers by counteracting the ionized polymers. Camphorsulfonic acid (CSA) [52,56,57,68–72] and HA [54,61,73] are commonly used as dopants for PANi and PPy, whereas poly(4-styrenesulfonate) (PSS) is commonly used for PEDOT [67,74–76].

PANi, PPy, and PEDOT confer semiconductor features ($\sigma = 10^{-3}$–10^{1} S/m; $Z = 10^{2}$–10^{5} Ω·m) and mechanical strength to biomaterials (Tables 1–4). The degradation [54–56,59,63,68] and swelling [54,57,58,60,63,65,67] of biomaterials are also reduced in the presence of hydrophobic conducting polymers. Interestingly, despite the hydrophobic nature of PANi, PPy, and PEDOT, the surface hydrophilicity of hydrophobic PLLA, PLA, and PCL biomaterials is improved with the addition of conductive polymers [61,70,77]. Although the latter properties can be perceived as drawbacks or advantages for the application of these electroactive biomaterials, the harsh conditions used for monomer polymerization are a major drawback. The acidic synthesis conditions are associated with the lysis of soft polymers, such as GEL [72] and possibly GG [58], affecting the mechanical properties of the electroactive biomaterials. Acidic reagents and unreacted monomers are also associated with cytotoxic effects. To overcome these issues, films [56,68,77], electrospun meshes [70–72], scaffolds [52,59], and matrices [58,60] have been purified through dialysis prior use. In fact, the use of already purified conducting polymers [78] to prepare hydrogels allows cell encapsulation that would be impossible in the

Table 3. Cell Responses to Electroactive Biomaterials and Electrical Fields in Neural Tissue Engineering[a]

Electroactive biomaterials					
Electroactive biomaterial	Other biomaterials	Electrical features	Cell type	Cellular response	Refs
GR; 0.1–4%	PDA, RGD, and PCL	$\sigma = 10^{-1}$ S/m	rSCs	↑ Expression of proliferative (ki67, BrDU), adhesion (N-cadherin and vinculin) and SCs (S100) proteins, co-culture mediated ↑ expression of neuron (Tuj1) and astrocyte (GFAP) proteins (relative to pristine)	[110]
GR; 1–4%	SF	–	miPSCs	↑ Cell differentiation towards neurons through ↑ expression of neuronal (TuJ, NeuN, GAP43) genes and/or proteins, ↑ cell differentiation towards astrocytes through ↑ expression of astrocyte (GFAP) genes and/or proteins (relative to pristine)	[41]
rGO	PCL	–	PC12	↑ Cell proliferation, ↑ cell differentiation towards neurons through ↑ expression of neuron (GAP43) genes (relative to pristine)	[100]
f-MWCNTs 0.02–0.1%	PEGDA	CSC = 0.12 mC cm^{-2}	mNSCs	↑ Cell proliferation and neurite length (relative to pristine)	[43]
ANi dimer; 10–40%	GEL	$\sigma = 10^{-3}$ S/m	PC12	Cell attachment and neurite extension, ↑ metabolic activity (relative to pristine)	[63]
ANi pentamer; 5–15%	PU and PGS	$\sigma = 10^{-3}$ S/m	rSCs RSC96	↑ Expression of myelinating SC-related genes (*KROX20*, *PMP22*), ↓ expression of immature SC-related genes (*NCAM*), ↑ expression of neurotrophic factors (NGF, BDNF) (relative to pristine)	[68]
PPy; 0.15–2.5%	TA	$\sigma = 10^{1}$ S/m	mNSCs	↑ NSCs differentiation into neurons through ↑ expression of neuron (Tuj1) proteins and ↓ expression of astrocyte (GFAP) proteins (relative to pristine)	[65]
PEDOT; 0.01 M	HA, PLLA and Lam	$\sigma = 10^{0}$ S/m	PC12	↑Cell viability, adhesion, and neurite length (relative to pristine)	[61]
PEDOT; 0.4 M	CHT and GEL	$\sigma = 10^{0}$ S/m $Z = 10^{2}\ \Omega \cdot m$	rNSCs	↑ Cell adhesion and proliferation, ↑ cell differentiation towards neurons and/or astrocytes through ↑ expression of neuron (Tuj1) and astrocyte (GFAP) genes and/or proteins and ↓ expression of oligodendrocytes (O4) genes and/or proteins (relative to pristine)	[53]
PEDOT; 8%	PU and LCGO	$\sigma = 10^{4}$ S/m	hNSCs	↑ Cell differentiation towards neurons and/or astrocytes through ↑ expression of neuron (Tuj1) and astrocyte (GFAP) proteins (relative to pristine)	[67]
PEDOT; 0%–10%	HA, CHT, and GEL	$\sigma = 10^{-1}$ S/m	PC12	↑ Cell viability and adhesion, ↑ expression of synapse growth genes (*GAP43* and *SYP*) (relative to pristine)	[54]
PEDOT; 25%	BC	–	PC12	↑ Cell orientation (relative to pristine)	[66]
PEDOT; N/A	HA, CHT, and GEL	$Z = 10^{3}\ \Omega \cdot m$	rNSCs	↑ Cell proliferation, ↑ cell differentiation towards neurons and/or astrocytes through ↑ expression of neurons (Tuj1) and astrocyte (GFAP) genes and/or proteins, ↓ expression of oligodendrocytes (O4) genes and/or proteins (relative to pristine)	[73]

(Continued on next page)

Table 3. ***Continued***

Electroactive biomaterials					
Electroactive biomaterial	**Other biomaterials**	**Electrical features**	**Cell type**	**Cellular response**	**Refs**
PVDF; 16% r-GR MWCNTs	PEI and PLO/Fbn	–	mNSCs	Differentiation towards neurons, astrocytes, and oligodendrocytes, ↑ differentiation towards neurons and/or oligodendrocytes through ↑ expression of neuron (Tuj1) and oligodendrocyte (O4) markers, ↑ synaptic boutons, ↑ oligodendrocytes branching (relative to pristine)	[101]
β-PVDF; 15%	–	–	mkNSCs	Differentiation towards neurons and/or astrocytes through ↑ expression of neuron (βIII-tubulin) and astrocyte (GFAP) markers	[82]
β-PVDF	–	d = −30±2 pC/N	PC12	↑ Neurite extension mediated by dynamic stimulation of PVDF by ultrasonic waves that activate Ca^{2+} channels via cAMP-dependent pathway (in relation to α-PVDF)	[83]
PVDF-TrFE; 20%	–	–	rSCs	SC growth and orientation and neurite extension and myelination (in co-culture with dorsal root ganglions)	[85]
Electrical fields					
DC					
Electrical field	**Electroactive biomaterial**	**Cell type**	**Cellular response**		**Refs**
U = 0.1 V/cm; Δt = 4 h/day for 7 days	PPY and PLCL	PC12	↑ Neurite length and expression of neurotrophic factors proteins (GDNF, BDNF, NT-3) (relative to nonstimulated cells)		[106]
AC					
Electrical field	**Electroactive biomaterial**	**Cell type**	**Cellular response**		**Refs**
Rectangular wave; U = 0.040 V; Δt = 30 min	PPy and PLA	PC12	↑ Neurite outgrowth and viability, ↑ cell differentiation towards neuron phenotype through ↑ expression of neuron (NF-200) proteins (relative to nonstimulated cells)		[108]
U = 0.1 V ω = 50 Hz Δt = 10 min/day for 15 days	GR	rMSCs-SCs	↑ Cell differentiation towards SC phenotype, expression of Schwann-related proteins (p75, s100, s100β) and release of neurotrophic factors (NGF) (relative to nonstimulated cells)		[104]
U = 0.1–0.5 V ω = 1–5 Hz Pulse width = 1 μs Δt = 1–3 days	GR	hBMSCs	↑Cell differentiation towards neurons through ↑ expression of neuron (MAP2 and β3-tubulin) proteins (relative to nonstimulated cells)		[102]
Monophasic wave U = 0.6 V ω = 0.1 Hz Pulse width = 1–100 ms Δt = 24 h	PEDOT and BC	PC12	↑ Cell orientation and action potential (relative to nonstimulated cells)		[66]
Monophasic wave U = 0.03 mA ω = 1 Hz Δt = 1 day	PEDOT and GO	rMSCs	↑ Proliferation, ↑ cell differentiation towards neurons and/or astrocytes through ↑ expression of neuron (Tuj1) and astrocyte (GFAP) proteins (relative to nonstimulated cells)		[103]

(Continued on next page)

Table 3. ***Continued***

AC				
Electrical field	**Electroactive biomaterial**	**Cell type**	**Cellular response**	**Refs**
Biphasic wave U = 0.1–1 mA ω = 100 Hz Pulse width = 100 μs Δt = 4 days	f-MWCNTs and PEGDA	NE-4C mNSCs	↑ Cell viability, ↑ cell differentiation towards neurons and/or astrocytes through ↑ expression of neuron (Tuj-1) and astrocyte (GFAP) proteins (relative to nonstimulated cells)	[43]
Biphasic wave U = 0.25 mA/cm^2 ω = 250 Hz Pulse width = 100 μs Δt = 8 h/day for 3 days	PEDOT, LCGO, and PU	hNSCs	↑ Neurite length and neurite levels (relative to nonstimulated cells)	[67]
Monophasic wave I = 0.5–1 mA ω = 10 Hz Pulse width = 60 μs Δt = 2 h	PEDOT, HA, Lam, and PLLA	PC12	↑ Cell viability and expression of synapse growth genes (*GAP43* and *SYP*), ↑ neurite length dependent on stimulus (relative to nonstimulated cells)	[61]

[a]Abbreviations: ANi, aniline; BC, bacterial cellulose; BDNF, brain-derived neurotrophic factor; BrDu, bromodeoxyuridine; CS, chondroitin sulfate; DS, dextran sulfate; ERK, extracellular signal-regulated kinases; Fbn, fibronectin; f-CNTs, functionalized carbon nanotubes; f-MWCNTs, functionalized multi-walled carbon nanotubes; GDNF, glial cell line-derived neurotrophic factor; GFAP, glial fibrillary acidic protein; GAP43, growth-associated protein 43; GEL, gelatin; GFAP, glial fibrillary acidic protein; GO, graphene oxide; h, human; Krox20, early growth response protein 2; L929, mouse fibroblast cell line; Lam, laminin; LDH, lactate dehydrogenase; LGCO, liquid crystal graphene oxide; m, murine; mk, monkey; MAP-2, microtubule-associated protein 2; MSCs, mesenchymal stem cells; MSCs-SCs, mesenchymal stem cells primed towards Schwann cell lineage; N/A, not available; NE-4C, murine neural stem cells; NeuN, hexaribonucleotide-binding protein-3; NF200, neurofilament 200; NGF, nerve growth factor; NSCs, neural stem cells; NT-3, neurotrophin-3; P75, low-affinity nerve growth factor receptor; PANi, polyaniline; PC12, rat neuron-like pheochromocytoma cell line; PEDOT, poly(3,4-ethylenedioxythiophene); PEGDA, poly(ethylene glycol) diacrylate; PEI, polyethyleneimide; PGS, poly(glycerol sebacate); PLLA, poly(L-lactide); PPy, polypyrrole; PLO, polyornithine; PMMA, poly(methyl methacrylate); PMP22, peripheral myelin protein 22; PPy, polypyrrole; PSD-95, postsynaptic density protein 95; PVDF, polyvinylidene fluoride; PVDF-TrFE, poly(vinylidenefluoride-co-trifluoroethylene); PU, polyurethane; rGO, reduced graphene oxide; RGCs, retinal ganglion cell; RSC96, rat Schwann cell line; SCs, primary Schwann cells; SH-SY5Y, human neuroblast cell line; SYP, synaptophysin; TA, tannic acid; Tuj1, neuron-specific class III beta-tubulin; ↑, upregulation; ↓ downregulation.

presence of acidic dopants. Despite these concerns, implantation of the conductive polymers *in vivo* does not show undesirable inflammatory reactions, but inflammation and fibrous tissue encapsulation are still detected; thus, there are reservations about using conductive polymers [79]. Moreover, these synthetic polymers are not biodegradable, which might lead to *in situ* chronic inflammation or other adverse effects, as soon as the nonbiodegradable byproducts are leached. As used for metals/metalloids and GR and its derivatives, different strategies are applied to improve the biocompatibility of these polymers, but more evidence is needed to confirm their viability before clinical translational.

Piezoelectric Polymers

Piezoelectric polymers generate electrical charge in response to deformation. This property is related to the ability of polymers to form a crystalline structure in which electric dipoles are formed. This crystalline structure can be triggered using a process named poling (polarization), which generates an electrical field able to align polymer charges and form electric dipoles [80]. Upon application of mechanical stress, an asymmetric shift of charges occurs within the biomaterials, altering their electric polarization and generating electricity [80]. These electrical properties are unique since biomaterials can generate electrical fields without the application of exogenous electrical fields.

Table 4. Responses of Cells to Electroactive Biomaterials and Electrical Fields in Cardiac Tissue Engineering[a]

Electroactive biomaterials					
Electroactive biomaterial	Other biomaterials	Electrical features	Cell type	Cellular response	Refs
GNRs	GEL-MA and ALG	$Z = 10^4\ \Omega\cdot m$	rCFs, rCMs	↑ Cell adhesion and organization, ↑ cell–cell coupling, ↑ expression of cardiac proteins (Cx43), synchronous contraction (relative to pristine)	[36]
	GEL-MA	$Z = 10^3\ \Omega\cdot m$	rCMs	↑ Cell viability and adhesion, ↑ expression of cardiac proteins (α-SA, cx43, cTnI) proteins, ↑ calcium transients, synchronous beating (relative to pristine)	[35]
SiNWs	–	$\sigma = 10^2$ S/m	hiPSC-CMs	↑ Organization of sarcomeres, ↑ expression of cardiac proteins (α-SA, MYL2 and MYH/MYH6) (relative to pristine)	[38]
GR	–		hiPSC-CMs	↑ Myofibril ultrastructural organization, conduction velocity and calcium (relative to pristine)	[45]
	PEG and PMMA	$\sigma = 10^{-1}$ S/m	rCMs	↑ Myofibrils and sarcomeres, ↑ expression of cardiac proteins (Cx43, SERCA2) and calcium-handling proteins, ↑ cell–cell coupling, ↑ action potential duration and peak calcium release (relative to pristine)	[117]
GR; 0.01%	PCL	$\sigma = 10^{-8}$ S/m $Z = 10^2\ \Omega\cdot m$	mESC-CMs	↑ Expression of cardiac proteins (Cx43, MHC, cTNT), ↑ synchronized contraction, calcium handling (relative to pristine)	[114]
GO; 0.05–0.9%	COL	$\sigma = 10^{-3}$ S/m	rCMs HUVECs	↑ Expression of cardiac genes (*Cx43*, *Actin4*, *Trpt2*) (CMs) (relative to pristine)	[51]
CNTs; 0.15 %	PCL and SF	–	rCMs ECs	↑ Expression of cardiac genes (*aSA* and *Cx43*) (relative to pristine)	[118]
f-MWCNTs	GEL-MA	$\sigma = 10^{-5}$ S/m $Z = 10^4\ \Omega\cdot m$	mMSCs-CMs	↑ Cell differentiation mediated by ↑ expression of cardiac genes and proteins (cTnT-2, NKx2-5, α-SA), synchronous beating (relative to pristine)	[115]
f-MWCNTs; 0.05–1%	–	$\sigma = 10^{-3}$ S/m $Z = 10^5\ \Omega\cdot m$	mMSCs-CMs	↑ Cell differentiation and expression of cardiac-related markers (Nkx2–5, Myh7, Trp-2, Gata4, Tbx5, Actg2, Acta2) (relative to pristine)	[116]
f-MWCNTs; 1–6 %	PELA	$\sigma = 10^0$ S/m	rCMs	↑ Expression of cardiac proteins (α-SA and cTnI), synchronous beating (relative to pristine)	[119]
ANi tetramer; 0.1 M	PU and Siloxane	$\sigma = 10^{-2}$ S/m	C2C12 HL-1	Proliferation and myotube formation (C2C12), ↑ expression of cardiac genes (*cx43*, *Trp2* and *SERCA*) and proteins (cx43, α-SMA, HL-1), calcium transient propagation (HL-1) (relative to pristine)	[56,57]
ANi pentamer; N/A	PLA	$\sigma = 10^{-3}$ S/m	H9c2	Cell adhesion and/or spread	[77]
PANi; 1.5–3%	–	$\sigma = 10^{-5}$ S/m	H9c2	↑ Cell–cell interaction, amount of myotubes, myotube length, cell orientation, expression of cardiac proteins (α-SA and cx43), synchronous beating (relative to pristine)	[70]

(Continued on next page)

Table 4. *Continued*

Electroactive biomaterials					
Electroactive biomaterial	Other biomaterials	Electrical features	Cell type	Cellular response	Refs
PVDF-TrFE	–	–	mESC-CMs mESC-ECs	Expression of cardiac proteins (cTnT, cx43, MHC) ↑ calcium handling, synchronous beating	[86]
Electrical fields					
AC					
Electrical field	Electroactive biomaterial		Cell type	Cellular response	Refs
ω = 0.5–2 Hz	GR and PCL		mESC-CMs	Synchronous beating modulated (↓) by electrical stimulation parameters	[114]
U = 3 V/cm ω = 1 Hz Pulse width = 10 ms Δt = 2 days	f-MWCNTs		mMSC-CMs	↑ Expression of cardiac proteins (Nkx2–5, Myh7, cTnT2, Gata4, Tbx5, Actg2), ↑ beating area	[116]
U = 3 V ω = 1 Hz Pulse width = 10 ms Δt = 2 days	f-MWCNTs and GEL-MA		mMSC-CMs	↑ Expression of cardiac genes and/or proteins (cTnT-2, NKx2-5, α-SA), ↑ synchronous beating area and frequency (relative to nonstimulated cells)	[115]
Biphasic wave U = 3 V/cm ω = 3–6 Hz Pulse width = 1 ms Δt = 7 days	COL		hiPSC-CMs	↓ Cell proliferation, ↑ expression of genes associated with potassium transients (KCNJ2), ↑ calcium handling, ↑ degree of structural and electrophysiological maturation, ↑ nonspontaneous beating, ↓ spontaneous beating (relative to nonstimulated cells) dependent on stimulation rate	[113]
U = 3.75 V/cm ω = 1 Hz Δt = 9 days	Si NWs		hiPSC-CMs	↑Cell–cell junction formation, ↑ organization of sarcomeres ↑ expression of cardiac genes and/or proteins (cx43, α-SA, cTnI, MYL2, MLC-2v), ↓ expression of genes associated with potassium channels (*HCN4*, *KCNJ2*), ↑ development of contractile machinery, ↓ spontaneous beat rate (relative to nonstimulated cells)	[38]
U = 5 V ω = 1 Hz Pulse width = 500 ms Δt = 6 days	PANi and PLLA		H9c2	↑ Cell proliferation ratio, ↑ intracellular calcium concentration (relative to nonstimulated cells), pseudopodia-like structure cell morphology after electrical stimulation	[77]
U = 2–10 V ω = 1–3 Hz Pulse width = 2 ms	GNRs and GEL-MA		rCMs	Synchronous beating modulated (↓) by electrical stimulation parameters (relative to nonstimulated cells)	[35]

[a]Abbreviations: α-SA, α-sarcomeric actin; α-SMA, α-smooth muscle actin; Actin4, actinin α 4; ACGT2, actin, gamma 2, smooth muscle, enteric; ALG, alginate; ANF, atrial natriuretic peptide; ANi, aniline; C2C12, mouse myoblast cell line; CFs, cardiac fibroblasts; CMs, cardiomyocytes; cTn2, cardiac troponin 2; cTnI, cardiac Troponin I; cTnT, cardiac troponin T; Cx43, connexin 43; ESC-CMs, embryonic stem cell-derived cardiomyocytes; f-MWCNTs, functionalized multiwalled carbon nanotubes; Gata4, GATA binding protein 4; GEL-MA, gelatin methacrylate; GNRs, gold nanorods; h, human; HCN4, hyperpolarization-activated cyclic nucleotide gated potassium channel 4; HL-1, proliferating cardiomyocyte cell line from mouse atrial tumors; HUVEC, human umbilical vein endothelial cells; H9c2, rat myoblast cell line; iPSC-CMs, induced pluripotent stem cell-derived cardiomyocytes; KCNJ2, potassium voltage-gated channel subfamily J member 2; m, mouse; MHC, major histocompatibility complex; MLC-2v, ventricular myosin light chain; MSCs, mesenchymal stem cells; MSC-CMs, mesenchymal stem cells primed to cardiomyocytes; MYH, myosin heavy chain; MYL, myosin light chain; NKx2-5, NK2 homeobox 5; NPPA/B, natriuretic peptide precursor A/B; NWs, nanowires; PANi, polyaniline; PEGDA, poly (ethylene glycol) diacrylate; PELA, poly(ethylene glycol)-poly(D,L-lactide) copolymer; PES, polyethersulfone; PLLA, poly(L-lactide); PMMA, poly(methyl methacrylate); PPy, polypyrrole; PVDF-TrFE, poly(vinylidenefluoride-co-trifluoroethylene); PU, polyurethane; r, rat; SERCA, sarco/endoplasmic reticulum Ca^{2+}-ATPase; Si, silicon; TA, tetraniline; Tbx5, T-box 5; Trp-2, troponin 2; TrpT-2, troponin T type 2; U, voltage; USSC, unrestricted somatic stem cells; Ω, frequency; Δt, time variation; ↑, upregulation; ↓ downregulation.

Piezoelectric features can be found in different synthetic polymers, including polyurethane (PU, 600 pC/N), polyvinylidene fluoride (PVDF, –32 pC/N), polyvinyl chloride (PVC, 5 pC/N), polyamide (nylon, 3 pC/N), and polypropylene glycol (PPG, 0.1 pC/N) [2]. To our knowledge, only the piezoelectric features of PVDF have been explored for TERM (Tables 1–4, Figure 1). The thermoplastic polymer PVDF has at least five possible crystalline forms (α, β, γ, δ, and ε), of which α and β are the most common [81–84]. Although α-PVDF is the most thermodynamically favorable form, it does not present piezoelectric properties. Piezoelectricity (–32 and –28 pC/N) is found in the β crystallization form of PVDF and its copolymer poly(vinylidenefluoride-co-trifluoroethylene) (PVDF-TrFE), although in a more favorable thermodynamic manner in the latter [2,33,81,83,85–87]. Depending on the dipole arrangement, a positive or negative net charge can be produced at the surface of PVDF membranes. The negative charges influence the behavior of the cell because of the higher adhesion of cations and proteins to PVDF membranes. They control the adhesion of cells through their negatively charged cell membranes [81,87]. PVDF is currently used as medical suture because of its long-term mechanical and chemical stability in the mild hydrolytic environment *in vivo*, evidencing good biocompatibility and anastomosis with the tissue [88].

Polyhydroxybutyrate (PHB) and poly(L-lactic acid) (PLA) are natural polymers being explored as more biodegradable piezoelectric polymers (Tables 1–4, Figure 1). PLA has four crystalline conformations, of which the β form presents piezoelectricity (10 pC/N) [2]. Interest in the piezoelectric features of PLA first arose in 1996, when Fukada *et al.* showed enhanced bone formation with drawn (piezoelectric) but not with undrawn (nonpiezoelectric) PLA [89]. It is hypothesized that movements of the cat leg generated a piezoelectric current, which aided bone formation [89]. PLA is already used in the USA as bone implants and soft tissue fillers [90,91] and is considered biocompatible and safe [92]. However, foreign body reactions and adverse inflammatory reactions have also been clinically reported [92]. PLA is biodegraded by hydrolysis into acidic products (lactic acid and glycolic acids) at a low degradation rate (1–5 years), which might result in delayed and adverse inflammatory reactions if the surrounding tissue does not efficiently eliminate the accumulation of acidic byproducts [92].

PHB presents a lower piezoelectric coefficient (1.3 pC/N) [2]. PHB piezoelectricity results from alterations in the PHB surface charge, with reported effects on cell adhesion and capsule adsorption on PANi-doped PHB/PCL electrospun fibers [93]. The potential for PHB piezoelectricity *in vivo* is still to be investigated, but the biodegradability and biocompatibility of PHB makes it an attractive material for use in TERM. PHB biodegrades by surface erosion, temperature, and hydrolysis, with degradation rates that vary from weeks to years. It is also considered biocompatible, given that PHB and its byproduct, 3-hydroxybutyric acid, exist in human plasma [94,95].

Progress in Electroactive Biomaterials and Electrical Stimulation

Neural Tissue

The adult mammalian central nervous system (CNS) cannot regenerate following an injury or insult, because of the inability of neurons to undergo axonal regeneration and the inhibitory repressive CNS microenvironment [96]. This is a major burden for patients who suffer stroke, traumatic brain injury or spinal cord injury, who generally only show limited recovery of function. Hence, there are high expectations particularly in the development of neural tissue engineering (TE) constructs for the repair of spinal cord injuries [97]. Axonal growth is observed in spinal cord injuries after implantation of conduits loaded with neurons, repairing Schwann cells or stem cells primed to these lineages [97]. Moreover, hollow tubes filled with fibers, filaments, gels, or sponges can support the survival, growth, and function of neural cells and guide axon growth [97]. Given the importance of biomaterial conductivity to maintain electrical communication between electroactive cells, action potentials, and nerve outgrowth, electroactive features are being added to biomaterials (Table 3).

Neuronal stem cells (NSCs) are the cells of preference to be used in neural TE due to their high neural differentiation ability. However, NSC are difficult to harvest because they only occur in the brain or spinal cord [98]. In addition, mesenchymal stem cells (MSC) show promise for use in neural TE strategies owing to their easy and high availability [99]. They have regenerative ability and multilineage

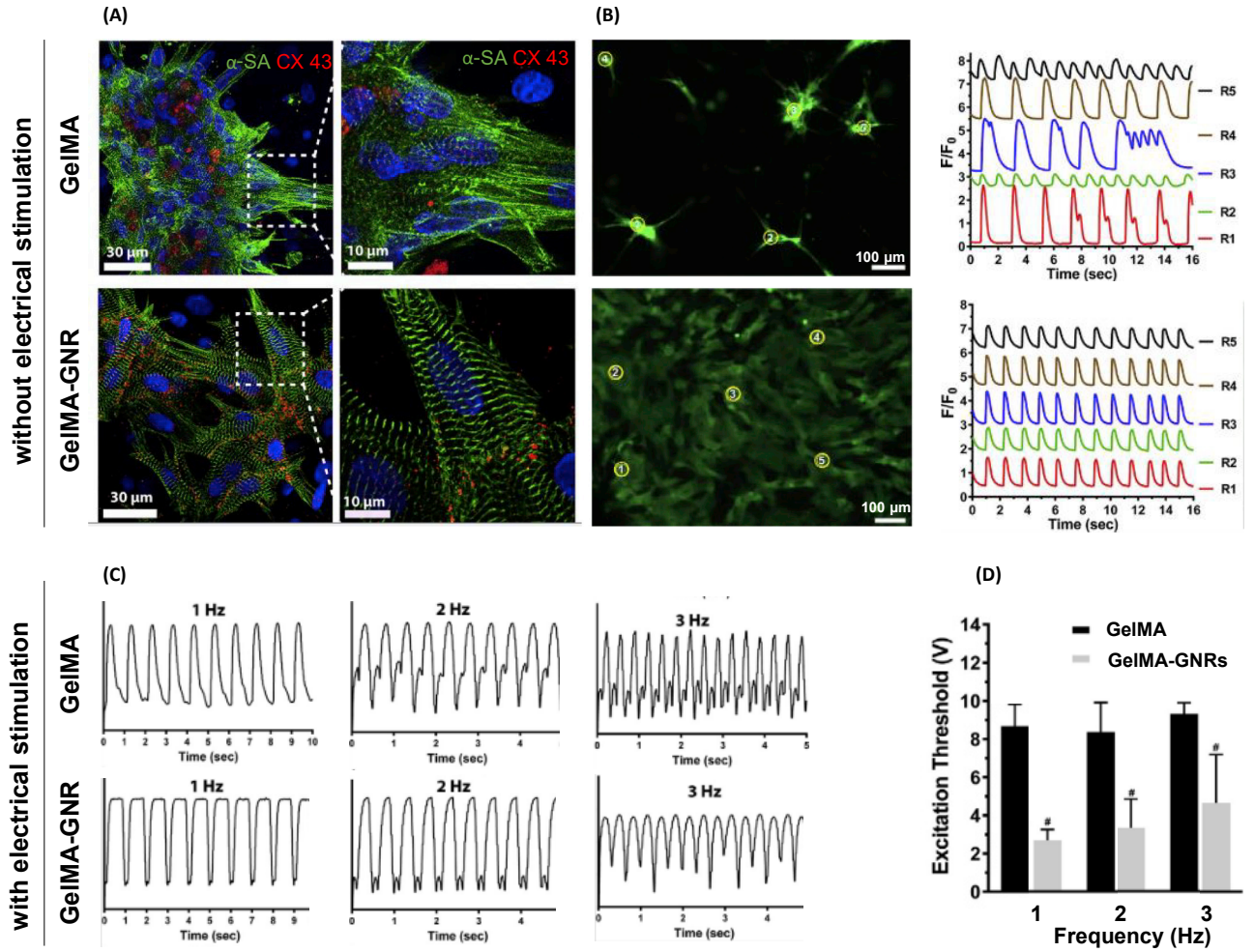

Figure 2. Cardiomyocyte Maturation and Beating on Gold Nanorod (GNR)-Loaded Gelatin Methacrylate (GelMA) Hydrogels with and without Electrical Stimulation.

(A) Immunostaining of the cardiac-specific markers sarcomeric α-actinin (α-SA, green) and connexin 43 (CX 43, red) after 7 days of neonatal rat ventricular cardiomyocyte culture on GelMA and GelMA-GNR hydrogels (arrows showing sarcomere formation). (B) Calcium transient and extracted related frequency signals of intracellular change in concentration of calcium within cultured cardiomyocytes in GelMA and GelMA-GNR hydrogels. R1–R5 represent regions 1–5. (C) Modulation of cardiomyocyte beating on GelMA and GelMA-GNR using electrical stimulation of different frequencies. (D) Excitation thresholds (i.e., minimum required voltage to induce synchronous contractions) of cardiomyocytes on GelMA and GelMA-GNR at different frequencies (#$P < 0.05$). Adapted, with permission, from [35].

differentiation capacity into different neural cell lineages, including neurons, astrocytes, oligodendrocytes, and Schwann cells [98,99]. Thus, the use of a single cell source that gives rise to different cell lineages is of value for generating a more complex neural TE construct.

The ability of NSCs to undergo multilineage differentiation is preserved in electroactive biomaterials, differentiating mainly towards neurons [41,53,65,67,73,82,100,101] and astrocytes [41,53,67,73,82,101], and triggered by exogenous electrical fields [43]. The impact of electrical stimulation appears to be greater on MSC differentiation because they are able to differentiate towards neurons [102] and astrocytes [103] without the need for exogenous biochemical agents. The differentiation of MSCs towards astrocytes [103] and Schwann cells [104] is also evident after electrical stimulation under standard neurogenic culture conditions. Although multilineage differentiation is important to generate complex neural TE constructs, control over the fate of stem cell differentiation can be

vital for strategies that envision the application of neurons or Schwann cells with particular functions. The ability of stem cells to differentiate towards a particular cell type was detected after culturing of NSCs in a tannic acid/PPy-based hydrogel [65]. Implantation of this construct in peripheral nerve defect resulted in the recovery of locomotor function through the activation of endogenous NSC neurogenesis towards Schwann cells and neurons at the lesion site [65].

Neurons are electrical excitable cells of the neural tissue that are able to generate synapses [105]. Increased neurite lengths are found in both conductive [43,61] and piezoelectric [83,85] biomaterials, and upon application of external electrical fields [61,67,106–108]. Some electroactive biomaterials are able to support the synaptic function of neurons [54,101], but electrical stimulation appears to improve the synaptic functions of neurons further because it promotes the generation of action potentials [66]. Moreover, the electrical stimulation of engineered constructs implanted in nerve defects was found to enhance nerve regeneration and functional recovery, possibly mediated by increased levels of neurotrophic factors, neurons, and Schwann cells found in the injured area [106].

Schwann cells exist in the peripheral nervous system and produce a myelin sheath around neurons to insulate them, enabling the propagation of synapses (myelinating Schwann cells). In response to injury, Schwann cells dedifferentiate into non-myelinating Schwann cells, which phagocyte damaged neurons and guide the growth of regenerating axons [109]. The myelinating Schwann cell phenotype is preserved in electroactive biomaterials as evidenced by the enhanced expression of neurotrophic factors and myelinating-related genes and/or proteins, and the ability to myelinate neurons [68,85,110]. Moreover, implantation of Schwann cell-containing TE constructs resulted in enhanced peripheral nerve repair mainly by improving axonal regrowth, remyelination, and recovery of cell electrophysiology [110,111]. Although the ability of electroactive biomaterials to promote the myelinating Schwann cell phenotype can be beneficial to insulate nerves *in vivo*, implantation of immature Schwann cells with regenerative capacity can be advantageous. However, this requires further investigation.

Cardiac Tissue

The most efficient treatment for myocardial infarction still relies on heart transplantation, which is hampered by limited availability and donor suitability [112]. Recreation of a contractile vascular muscle heart *in vitro* is a promising approach to substitute the damaged tissue and restore normal cardiac function [112]. Strategies to develop cardiovascular TE constructs focus on the use of instructive and elastomeric biomaterials to support the growth, maturation, and contraction of cardiomyocytes (CMs). *In vitro* vascularization of the construct is also targeted with the use of particular cells and technologies [112]. Given that electroactive myocytes are responsible for heart contraction, it is relevant to use electroactive biomaterials to engineer cardiac TE constructs to sustain cell electrophysiology (Table 4). The application of external electric fields is also useful to modulate CM contraction (Table 2).

The differentiation of iPSCs [38,45,113], ESCs [86,114], and MSCs [115,116] towards CMs is possible with the use of appropriate cell culture conditions. Electroactive biomaterials sustain and stimulate the differentiation of stem cells towards CMs at a level similar to primary CMs or even those observed with cell lines. In addition, the number of myotubes, myofibrils, and sarcomeres [56,57,70,117], myofibril and/or sarcomere organization [38,45], cell-to-cell coupling [36,117], and cardiac gene and/or protein expression [35,36,38,51,56,57,114–119] are upregulated in electroactive biomaterials compared with pristine biomaterials. Calcium handling [35,45,56,57,114,117] and the spontaneous and synchronous contractions of CMs [35,36,114,115,119] are also improved in electroactive biomaterials but not in pristine biomaterials (Figure 2). Moreover, the heart function of rats was found to be improved when treated with CM-laden electroactive hydrogels compared with pristine biomaterials [47]. Application of external electrical fields is able to further improve CM differentiation in relation to nonstimulated cells (Figure 2) [35,38,77,113–116]. Interestingly, the external fields are not only able to modulate the contraction rate, but also capable of reducing spontaneous contraction and triggering electric field-mediated contraction.

Skeletal Muscle Tissue

The regenerative process in the muscle is efficient due to the presence of satellite cells and resident quiescent myoblasts with stem cell multipotency that are able to go through myogenic differentiation in response to injury. However, the regenerative capacity of satellite cells is limited to small muscle injuries since stem cells are unable to regenerate large muscle damage, such as volumetric muscle loss [120]. Hence, TE strategies focus on the development of vascularized innervated muscle engineered tissues to restore muscle functionality [120]. Primary muscle satellite cells are the most appropriate cells to use to engineer skeletal muscle TE constructs, but their reduced expansion is a limiting factor [121]. Thus, research has focused on the myogenic differentiation of MSC, although with little success so far [122]. An immortalized cell line of mouse myoblasts (C2C12) has also been used as an alternative approach. Biomaterials for skeletal muscle TE comprise specific features, such as anisotropy to promote the alignment needed for myoblasts to fuse into myotubes; elasticity to sustain muscle contractility; and conductivity to trigger cell electrophysiology and response to electrical fields (Table 2).

C2C12 cell differentiation is increased in electroactive biomaterials in relation to pristine biomaterials [46,50,58,59,72,87,123]. Cell fusion into myotubes [46,50,87,123] and the expression of myogenic genes and/or proteins [46,50,58,59,72,87,123] are commonly achieved in electroactive biomaterials. Despite being explored to a lower extent, murine satellite muscle cells show similar results [71,124]. Electrical fields also have an important role in the electrophysiological function of C2C12 cells [72,125–127]. Application of AC resulted in calcium transients [72,125] and myotube contraction [72,125–127], in some cases modulated by frequency [127].

MSC myogenic differentiation is an exciting approach that may be investigated further as a more reliable cellular alternative for TERM. To our knowledge, only Björninen and colleagues have explored the ability of electroactive biomaterials and electrical stimulation to prompt human adipose-derived MSCs (ASCs) for myogenic differentiation [128]. These cells were able to express calponin and myosin heavy chain (MHC) myogenic proteins after culture in poly(trimethylene carbonate) (PTMC)/PPy scaffolds using smooth muscle differentiation medium. However, the levels of differentiation were not improved with electrical stimulation.

Bone

There is a need for a bone implant that restores the loss or dysfunctional bone tissue caused by critical bone defects resulting from bone fractures or bone-related diseases, such as osteoporosis and osteoarthritis [129]. Strategies of TE focus on recreating the vascularized bone tissue *in vitro* through the use of hard, porous, osteoinductive, osteoconductive, and osteopromotive biomaterials loaded with bone-forming cells and endothelial cells to ultimately re-establish the mechanical stability of the skeletal tissue and promote bone formation [129]. Until recently, the design of biomaterials for bone TE had disregarded electrical conductive cues since primary bone cells are not electrically excitable *per se*. However, the awareness of bone piezoelectric features has boosted the investigation of electrical fields in bone cells [26]. Osteogenic differentiation triggered by electrical fields highlights the need to include electrical conductivity in the list of features required in biomaterials for bone TE, and electrical stimulation as a tool to improve osteogenic differentiation (Table 1).

Piezoelectric biomaterials are being explored for bone TE due to the piezoelectric nature of bone. BMSC osteogenic differentiation was observed in polarized PVDF-Ti films but not in nonpolarized membranes, even in the absence of a osteogenic cocktail medium [81]. These results were further supported by an *in vivo* study that showed superior bone growth in rat calvarial bone defects after treatment with PVDF-TrFE/$BaTiO_3$ membranes and osteoblastic cells (OBs) differentiated from BMSCs [33].

OBs and MSCs primed to the osteogenic lineage (MSC-OBs) are also being explored for bone TE. Osteogenic differentiation is achieved by culturing these cells in an osteogenic cocktail medium. Under standard osteogenic culture conditions, both electroactive biomaterials [32,52,74,81,84] and

electrical fields [31,130–141] trigger osteogenic differentiation. Electrical stimulation appears to have a major role, because BMSCs are able to differentiate towards the osteogenic lineage even in the absence of a osteogenic cocktail medium [81,102,138,142]. Further osteogenic differentiation is also detected with electrical stimulation under standard osteogenic culture conditions, as evidenced by the enhanced alkaline phosphatase activity [131,133,136,139,140], calcium deposition [31,131–134,137,138,140], and expression of osteogenic genes and/or proteins [31,130,133,135,137,139,141].

Outstanding Questions

How do electrical fields affect cellular behavior?

Which cellular signaling pathways are activated?

Is the cellular response permanent or transient?

Is the functionality of the electrostimulated mature biological tissues (e.g., skeletal muscle and cardiac tissue contractility) preserved after implantation *in vivo*?

Concluding Remarks and Future Perspectives

Engineering a construct that closely emulates the tissue that needs to repair and regenerate remains a major aim of TERM. Cellular, biochemical, and mechanical cues have long been considered in the development of biological tissues, but the importance of electrical features is only starting to be appreciated. Electric fields are more than an epiphenomenon in the human body; they are responsible for myriad physiological processes. Recent advances have shown the impact of using conductive substrates and/or matrices and exogenous electrical fields on the maturation of biological tissues for TERM. Electrical phenomena improve the maturation of bone and neural tissues and trigger the contraction of cardiac and skeletal muscles. However, there is an urgent need to better understand how these electrical phenomena affect cell behavior. Are these effects preserved in time or are they merely transitory (see Outstanding Questions)? Neural TE requires further investigation to modulate and trigger interneuronal communication *in vitro* through synapses. Tissues that are commonly exposed to electrical fields, such as skin after injury or tendons after mechanical stress, can also benefit from the use of electroactive biomaterials and/or electrical stimulation. Nevertheless, most of the results presented herein were from *in vitro* assays. Long-term analysis of the biodegradation and/or degradation byproducts and biocompatibility of these electroactive materials is essential to select the most promising material for TERM before clinical translational. Moreover, the development of realistic *in vivo* models that enable us to understand the efficacy of these strategies will further progress the area of electrical field-based TE strategies.

Acknowledgments

The authors acknowledge Tomé Silva for kind advice on electronics. This work is financially supported by POCI-01-0145-FEDER-007038-UMINHO/BPD/44/2016 (to L.P.d.S.), and European Union Framework Program for Research and Innovation Horizon 2020 on Forefront Research in 3D Disease Cancer Models as in vitro Screening Technologies (FoReCaST) under grant agreement no. 668983.

References

1. Messerli, M.A. and Graham, D.M. (2011) Extracellular electrical fields direct wound healing and regeneration. *Biol. Bull.* 221, 79–92
2. Fukada, E. (2000) History and recent progress in piezoelectric polymers. *IEEE Trans. Ultrason. Ferroelectr. Freq. Control* 47, 1277–1290
3. Langer, R. and Vacanti, J. (1993) Tissue engineering. *Science* 260, 920–926
4. Kirsner, R.S. (1998) The use of Apligraf in acute wounds. *J. Dermatol.* 25, 805–811
5. MacChiarini, P. *et al.* (2004) First human transplantation of a bioengineered airway tissue. *J. Thorac. Cardiovasc. Surg.* 128, 638–641
6. L'Heureux, N. *et al.* (2006) Human tissue-engineered blood vessels for adult arterial revascularization. *Nat. Med.* 12, 361–365
7. Atala, A. *et al.* (2006) Tissue-engineered autologous bladders for patients needing cystoplasty. *Lancet* 367, 1241–1246
8. Raya-Rivera, A. *et al.* (2011) Tissue-engineered autologous urethras for patients who need reconstruction: an observational study. *Lancet* 377, 1175–1182
9. Faes, T.J.C. *et al.* (1999) The electric resistivity of human tissues (100 Hz-10 MHz): a meta-analysis of review studies. *Physiol. Meas.* 20, R1–R10
10. Levin, M. (2007) Large-scale biophysics: ion flows and regeneration. *Trends Cell Biol.* 17, 261–270
11. Kadir, L.A. *et al.* (2018) Emerging roles of the membrane potential: action beyond the action potential. *Front. Physiol.* 9, 1–10
12. Buzsaki, G. and Draguhn, A. (2004) Neuroscience neuronal oscillations in cortical networks. *Science* 304, 1926–1938
13. Fröhlich, F. and McCormick, D.A. (2010) Endogenous electric fields may guide neocortical network activity. *Neuron* 67, 129–143
14. Chiappalone, M. *et al.* (2009) Low-frequency stimulation enhances burst activity in cortical cultures during development. *Neuroscience* 165, 692–704
15. Amin, H. *et al.* (2016) Electrical responses and spontaneous activity of human iPS-derived neuronal networks characterized for 3-month culture with 4096-electrode arrays. *Front. Neurosci.* 10, 121
16. Sendi, M.S.E. *et al.* (2018) Chronic electrical stimulation promotes the excitability and plasticity

of ESC-derived neurons following glutamate-induced inhibition *in vitro*. *Sci. Rep.* 8, 1–16
17. Zhao, Y. *et al.* (2014) High-frequency electrical stimulation suppresses cholinergic accumbens interneurons in acute rat brain slices through GABA B receptors. *Eur. J. Neurosci.* 40, 3653–3662
18. Yao, L. *et al.* (2011) Electric field-guided neuron migration: a novel approach in neurogenesis. *Tissue Eng. B Rev.* 17, 143–153
19. Kobelt, L.J. *et al.* (2014) Short duration electrical stimulation to enhance neurite outgrowth and maturation of adult neural stem progenitor cells. *Ann. Biomed. Eng.* 42, 2164–2176
20. Berger, H.J. *et al.* (1994) Continual electric field stimulation preserves contractile function of adult ventricular myocytes in primary culture. *Am. J. Physiol. Circ. Physiol.* 266, H341–H349
21. Chan, Y.C. *et al.* (2013) Electrical stimulation promotes maturation of cardiomyocytes derived from human embryonic stem cells. *J. Cardiovasc. Transl. Res.* 6, 989–999
22. Cai, W. *et al.* (2016) Electrical stimulation enhances cardiac differentiation of human induced pluripotent stem cells for myocardial infarction therapy. *Antioxid. Redox Signal.* 28, 371–384
23. Consolo, F. *et al.* (2013) Monophasic and biphasic electrical stimulation induces a precardiac differentiation in progenitor cells isolated from human heart. *Stem Cells Dev.* 23, 888–898
24. Nedachi, T. *et al.* (2008) Contractile C_2C_{12} myotube model for studying exercise-inducible responses in skeletal muscle. *Am. J. Physiol. Metab.* 295, E1191–E1204
25. Rustan, A.C. *et al.* (2012) Electrical pulse stimulation of cultured human skeletal muscle cells as an *in vitro* model of exercise. *PLoS One* 7, e33203
26. Isaacson, B.M. and Bloebaum, R.D. (2010) Bone bioelectricity: what have we learned in the past 160 years? *J. Biomed. Mater. Res. A* 95, 1270–1279
27. Özkucur, N. *et al.* (2009) Local calcium elevation and cell elongation initiate guided motility in electrically stimulated osteoblast-like cells. *PLoS One* 4, e6131
28. Clark, C.C. *et al.* (2014) Up-regulation of expression of selected genes in human bone cells with specific capacitively coupled electric fields. *J. Orthop. Res.* 32, 894–903
29. Creecy, C.M. *et al.* (2013) Mesenchymal stem cell osteodifferentiation in response to alternating electric current. *Tissue Eng. A* 19, 467–474
30. Kirsch, D.L. and Nichols, F. (2013) Cranial electrotherapy stimulation for treatment of anxiety, depression, and insomnia. *Psychiatr. Clin. North Am.* 36, 169–176
31. Park, J. *et al.* (2016) Electric field-induced osteogenic differentiation on TiO_2 nanotubular layer. *Tissue Eng. C Methods* 22, 809–821
32. Tang, Y. *et al.* (2017) Fabrication and *in vitro* biological properties of piezoelectric bioceramics for bone regeneration. *Sci. Rep.* 7, 1–12
33. Freitas, G.P. *et al.* (2017) Potential of osteoblastic cells derived from bone marrow and adipose tissue associated with a polymer/ceramic composite to repair bone tissue. *Calcif. Tissue Int.* 101, 312–320
34. Elahi, N. *et al.* (2018) Recent biomedical applications of gold nanoparticles: a review. *Talanta* 184, 537–556
35. Navaei, A. *et al.* (2016) Gold nanorod-incorporated gelatin-based conductive hydrogels for engineering cardiac tissue constructs. *Acta Biomater.* 41, 133–146
36. Zhu, K. *et al.* (2017) Gold nanocomposite bioink for printing 3D cardiac constructs. *Adv. Funct. Mater.* 27, 1605352
37. Gogurla, N. *et al.* (2016) Metal nanoparticles triggered persistent negative photoconductivity in silk protein hydrogels. *Nanoscale* 8, 7695–7703
38. Richards, D.J. *et al.* (2016) Nanowires and electrical stimulation synergistically improve functions of hiPSC cardiac spheroids. *Nano Lett.* 16, 4670–4678
39. Asri, R.I.M. *et al.* (2017) Corrosion and surface modification on biocompatible metals: a review. *Mater. Sci. Eng. C* 77, 1261–1274
40. Nair, M. and Elizabeth, E. (2015) Applications of titania nanotubes in bone biology. *J. Nanosci. Nanotechnol.* 15, 939–955
41. Niu, Y. *et al.* (2018) Enhancing neural differentiation of induced pluripotent stem cells by conductive graphene/silk fibroin films. *J. Biomed. Mater. Res. A* 106, 2973–2983
42. Singh, N. *et al.* (2016) Chitin and carbon nanotube composites as biocompatible scaffolds for neuron growth. *Nanoscale* 8, 8288–8299
43. Lee, S.J. *et al.* (2018) 3D printing nano conductive multi-walled carbon nanotube scaffolds for nerve regeneration. *J. Neural Eng.* 15, 016018
44. Chen, M. *et al.* (2017) Biodegradation of carbon nanotubes, graphene, and their derivatives. *Trends Biotechnol.* 35, 836–846
45. Wang, J. *et al.* (2017) Graphene sheet-induced global maturation of cardiomyocytes derived from human induced pluripotent stem cells. *ACS Appl. Mater. Interfaces* 9, 25929–25940
46. Du, Y. *et al.* (2018) Biomimetic elastomeric, conductive and biodegradable polycitrate-based nanocomposites for guiding myogenic differentiation and skeletal muscle regeneration. *Biomaterials* 157, 40–50
47. Zhou, J. *et al.* (2018) Injectable OPF/graphene oxide hydrogels provide mechanical support and enhance cell electrical signaling after implantation into myocardial infarct. *Theranostics* 8, 3317–3330
48. Costa, P.M. *et al.* (2016) Functionalized carbon nanotubes: from intracellular uptake and cell-related toxicity to systemic brain delivery. *J. Control. Release* 241, 200–219
49. Lalwani, G. *et al.* (2016) Toxicology of graphene-based nanomaterials. *Adv. Drug Deliv. Rev.* 105, 109–144
50. Patel, A. *et al.* (2016) Cell-instructive graphene-containing nanocomposites induce multinucleated myotube formation. *Ann. Biomed. Eng.* 44, 2036–2048
51. Norahan, M.H. *et al.* (2018) Electroactive graphene oxide-incorporated collagen assisting vascularization for cardiac tissue engineering. *J. Biomed. Mater. Res. A* 107, 204–219
52. Chen, J. *et al.* (2018) Conductive nanofibrous composite scaffolds based on *in-situ* formed polyaniline nanoparticle and polylactide for bone regeneration. *J. Colloid Interface Sci.* 514, 517–527
53. Wang, S. *et al.* (2018) 3D culture of neural stem cells within conductive PEDOT layer-assembled chitosan/gelatin scaffolds for neural tissue engineering. *Mater. Sci. Eng. C* 93, 890–901
54. Wang, S. *et al.* (2017) Hyaluronic acid doped-poly(3,4-ethylenedioxythiophene)/chitosan/gelatin (PEDOT-HA/Cs/Gel) porous conductive scaffold for nerve regeneration. *Mater. Sci. Eng. C* 71, 308–316
55. Xu, C. *et al.* (2017) Biodegradable and electroconductive poly(3,4-ethylenedioxythiophene)/carboxymethyl chitosan

hydrogels for neural tissue engineering. *Mater. Sci. Eng. C* 84, 32–43
56. Baheiraei, N. *et al.* (2016) Electroactive polyurethane/siloxane derived from castor oil as a versatile cardiac patch, part I: synthesis, characterization, and myoblast proliferation and differentiation. *J. Biomed. Mater. Res. A* 104, 775–787
57. Baheiraei, N. *et al.* (2016) Electroactive polyurethane/siloxane derived from castor oil as a versatile cardiac patch, part II: HL-1 cytocompatibility and electrical characterizations. *J. Biomed. Mater. Res. A* 104, 1398–1407
58. Srisuk, P. *et al.* (2018) Electroactive gellan gum/polyaniline spongy-like hydrogels. *ACS Biomater. Sci. Eng.* 4, 1779–1787
59. Zhang, M. and Guo, B. (2017) Electroactive 3D scaffolds based on silk fibroin and water-borne polyaniline for skeletal muscle tissue engineering. *Macromol. Biosci.* 17, 1–10
60. Berti, F.V. *et al.* (2017) Synthesis and characterization of electroactive gellan gum spongy-like hydrogels for skeletal muscle tissue engineering applications. *Tissue Eng. A* 23, 968–979
61. Wang, S. *et al.* (2017) Fabrication and characterization of conductive poly (3,4-ethylenedioxythiophene) doped with hyaluronic acid/poly (L-lactic acid) composite film for biomedical application. *J. Biosci. Bioeng.* 123, 116–125
62. Zhuang, A. *et al.* (2018) All-organic conductive biomaterial as an electroactive cell interface. *ACS Appl. Mater. Interfaces* 10, 35547–35556
63. Zarrintaj, P. *et al.* (2018) A facile route to the synthesis of anilinic electroactive colloidal hydrogels for neural tissue engineering applications. *J. Colloid Interface Sci.* 516, 57–66
64. Arioz, I. *et al.* (2018) Biocompatible electroactive tetra(aniline)-conjugated peptide nanofibers for neural differentiation. *ACS Appl. Mater. Interfaces* 10, 308–317
65. Zhou, L. *et al.* (2018) Soft conducting polymer hydrogels cross-linked and doped by tannic acid for spinal cord injury repair. *ACS Nano* 12, 10957–10967
66. Chen, C. *et al.* (2017) Electrically-responsive core-shell hybrid microfibers for controlled drug release and cell culture. *Acta Biomater.* 55, 434–442
67. Javadi, M. *et al.* (2018) Conductive tough hydrogel for bioapplications. *Macromol. Biosci.* 18, 1–11
68. Wu, Y. *et al.* (2016) Electroactive biodegradable polyurethane significantly enhanced Schwann cells myelin gene expression and neurotrophin secretion for peripheral nerve tissue engineering. *Biomaterials* 87, 18–31
69. Wu, Y. *et al.* (2018) Conductive micropatterned polyurethane films as tissue engineering scaffolds for Schwann cells and PC12 cells. *J. Colloid Interface Sci.* 518, 252–262
70. Wang, L. *et al.* (2017) Electrospun conductive nanofibrous scaffolds for engineering cardiac tissue and 3D bioactuators. *Acta Biomater.* 59, 68–81
71. Hosseinzadeh, S. *et al.* (2016) The nanofibrous PAN-PANi scaffold as an efficient substrate for skeletal muscle differentiation using satellite cells. *Bioprocess Biosyst. Eng.* 39, 1163–1172
72. Ostrovidov, S. *et al.* (2017) Gelatin-polyaniline composite nanofibers enhanced excitation-contraction coupling system maturation in myotubes. *ACS Appl. Mater. Interfaces* 9, 42444–42458
73. Wang, S. *et al.* (2017) Neural stem cell proliferation and differentiation in the conductive PEDOT-HA/Cs/Gel scaffold for neural tissue engineering. *Biomater. Sci.* 5, 2024–2034
74. Guex, A.G. *et al.* (2017) Highly porous scaffolds of PEDOT:PSS for bone tissue engineering. *Acta Biomater.* 62, 91–101
75. Chang, H.C. *et al.* (2016) Conductive PEDOT:PSS coated polylactide (PLA) and poly(3-hydroxybutyrate-co-3-hydroxyvalerate) (PHBV) electrospun membranes: fabrication and characterization. *Mater. Sci. Eng. C* 61, 396–410
76. Xu, Y. *et al.* (2018) Noncovalently assembled electroconductive hydrogel. *ACS Appl. Mater. Interfaces* 10, 14418–14425
77. Wang, Y. *et al.* (2018) Intracellular calcium ions and morphological changes of cardiac myoblasts response to an intelligent biodegradable conducting copolymer. *Mater. Sci. Eng. C* 90, 168–179
78. Petrov, P. *et al.* (2016) Novel electrically conducting 2-hydroxyethylcellulose/polyaniline nanocomposite cryogels: synthesis and application in tissue engineering. *Carbohydr. Polym.* 140, 349–355
79. Mattioli-Belmonte, M. *et al.* (2003) Tailoring biomaterial compatibility: *in vivo* tissue response versus *in vitro* cell behavior. *Int. J. Artif. Organs* 26, 1077–1085
80. Dineva, P.S. *et al.* (2014) Dynamic Fracture of Piezoelectric Materials: Solution of Time-Harmonic Problems via BIEM (Springer International Publishing)
81. Zhou, Z. *et al.* (2016) Polarization of an electroactive functional film on titanium for inducing osteogenic differentiation. *Sci. Rep.* 6, 1–8
82. Lins, L.C. *et al.* (2017) Effect of polyvinylidene fluoride electrospun fiber orientation on neural stem cell differentiation. *J. Biomed. Mater. Res. B Appl. Biomater.* 105, 2376–2393
83. Hoop, M. *et al.* (2017) Ultrasound-mediated piezoelectric differentiation of neuron-like PC12 cells on PVDF membranes. *Sci. Rep.* 7, 4028
84. Sobreiro-Almeida, R. *et al.* (2017) Human mesenchymal stem cells growth and osteogenic differentiation on piezoelectric poly(vinylidene fluoride) microsphere substrates. *Int. J. Mol. Sci.* 18, E2391
85. Wu, S. *et al.* (2018) Aligned fibrous PVDF-TrFE scaffolds with Schwann cells support neurite extension and myelination *in vitro*. *J. Neural Eng.* 15, 056010
86. Hitscherich, P. *et al.* (2016) The effect of PVDF-TrFE scaffolds on stem cell derived cardiovascular cells. *Biotechnol. Bioeng.* 113, 1577–1585
87. Ribeiro, S. *et al.* (2018) Electroactive biomaterial surface engineering effects on muscle cells differentiation. *Mater. Sci. Eng. C* 92, 868–874
88. Laroche, G. *et al.* (1995) Polyvinylidene fluoride monofilament sutures: can they be used safely for long-term anastomoses in the thoracic aorta? *Artif. Organs* 19, 1190–1199
89. Ikada, Y. *et al.* (1996) Enhancement of bone formation by drawn poly(L-lactide). *J. Biomed. Mater. Res.* 30, 553–558
90. Santoro, M. *et al.* (2016) Poly(lactic acid) nanofibrous scaffolds for tissue engineering. *Adv. Drug Deliv. Rev.* 107, 206–212
91. Ke, Y. *et al.* (2017) Reactive blends based on polyhydroxyalkanoates: preparation and biomedical application. *Mater. Sci. Eng. C* 70, 1107–1119

92. Ramot, Y. *et al.* (2016) Biocompatibility and safety of PLA and its copolymers. *Adv. Drug Deliv. Rev.* 107, 153–162
93. Timin, A.S. *et al.* (2018) Multifunctional scaffolds with improved antimicrobial properties and osteogenicity based on piezoelectric electrospun fibers decorated with bioactive composite microcapsules. *ACS Appl. Mater. Interfaces* 10, 34849–34868
94. Philip, S. *et al.* (2007) Polyhydroxyalkanoates: biodegradable polymers with a range of applications. *J. Chem. Technol. Biotechnol.* 82, 233–247
95. Reusch, R.N. *et al.* (1992) Transport of poly-β-hydroxybutyrate in human plasma. *Biochim. Biophys. Acta (BBA)/Lipids Lipid Metab.* 1123, 33–40
96. Fry, E.J. (2001) Central nervous system regeneration: mission impossible? *Clin. Exp. Pharmacol. Physiol.* 28, 253–258
97. Gu, X. *et al.* (2014) Neural tissue engineering options for peripheral nerve regeneration. *Biomaterials* 35, 6143–6156
98. Tang, Y. *et al.* (2017) Current progress in the derivation and therapeutic application of neural stem cells. *Cell Death Dis.* 8, e3108
99. Chamberlain, G. *et al.* (2007) Concise review: mesenchymal stem cells: their phenotype, differentiation capacity, immunological features, and potential for homing. *Stem Cells* 25, 2739–2749
100. Vijayavenkataraman, S. *et al.* (2018) 3D-printed PCL/rGO conductive scaffolds for peripheral nerve injury repair. *Artif. Organs* 43, 515–523
101. Defteralı, Ç. *et al.* (2016) *In vitro* evaluation of biocompatibility of uncoated thermally reduced graphene and carbon nanotube-loaded PVDF membranes with adult neural stem cell-derived neurons and glia. *Front. Bioeng. Biotechnol.* 4, 1–19
102. Balikov, D.A. *et al.* (2016) Directing lineage specification of human mesenchymal stem cells by decoupling electrical stimulation and physical patterning on unmodified graphene. *Nanoscale* 8, 13730–13739
103. Guo, W. *et al.* (2016) Self-powered electrical stimulation for enhancing neural differentiation of mesenchymal stem cells on graphene-poly(3,4-ethylenedioxythiophene) hybrid microfibers. *ACS Nano* 10, 5086–5095
104. Das, S.R. *et al.* (2017) Electrical differentiation of mesenchymal stem cells into Schwann-cell-like phenotypes using inkjet-printed graphene circuits. *Adv. Healthc. Mater.* 6, 1–8
105. Ye, H. and Steiger, A. (2015) Neuron matters: electric activation of neuronal tissue is dependent on the interaction between the neuron and the electric field. *J. Neuroeng. Rehabil.* 12, 1–9
106. Song, J. *et al.* (2016) Polymerizing pyrrole coated poly (L-lactic acid-co-ε-caprolactone) (PLCL) conductive nanofibrous conduit combined with electric stimulation for long-range peripheral nerve regeneration. *Front. Mol. Neurosci.* 9, 1–13
107. Zhou, X. *et al.* (2017) Enhancement of neurite adhesion, alignment and elongation on conductive polypyrrole-poly(lactide acid) fibers with cell-derived extracellular matrix. *Colloids Surfaces B Biointerfaces* 149, 217–225
108. Tian, L. *et al.* (2016) Synergistic effect of topography, surface chemistry and conductivity of the electrospun nanofibrous scaffold on cellular response of PC12 cells. *Colloids Surfaces B Biointerfaces* 145, 420–429
109. Jessen, K.R. and Mirsky, R. (2016) The repair Schwann cell and its function in regenerating nerves. *J. Physiol.* 594, 3521–3531
110. Qian, Y. *et al.* (2018) An integrated multi-layer 3D-fabrication of PDA/RGD coated graphene loaded PCL nanoscaffold for peripheral nerve restoration. *Nat. Commun.* 9, 323
111. Lee, Y.S. *et al.* (2017) Enhanced noradrenergic axon regeneration into schwann cell-filled PVDF-TrFE conduits after complete spinal cord transection. *Biotechnol. Bioeng.* 114, 444–456
112. Weinberger, F. *et al.* (2017) Engineering cardiac muscle tissue. *Circ. Res.* 120, 1487–1500
113. Sun, X. and Nunes, S.S. (2016) Biowire platform for maturation of human pluripotent stem cell-derived cardiomyocytes. *Methods* 101, 21–26
114. Hitscherich, P. *et al.* (2018) Electroactive graphene composite scaffolds for cardiac tissue engineering. *J. Biomed. Mater. Res. A* 106, 2923–2933
115. Ahadian, S. *et al.* (2016) Hybrid hydrogel-aligned carbon nanotube scaffolds to enhance cardiac differentiation of embryoid bodies. *Acta Biomater.* 31, 134–143
116. Ahadian, S. *et al.* (2017) Carbon nanotubes embedded in embryoid bodies direct cardiac differentiation. *Biomed. Microdevices* 19, 57
117. Smith, A.S.T. *et al.* (2017) Micro-and nano-patterned conductive graphene-PEG hybrid scaffolds for cardiac tissue engineering. *Chem. Commun.* 53, 7412–7415
118. Wu, Y. *et al.* (2017) Interwoven aligned conductive nanofiber yarn/hydrogel composite scaffolds for engineered 3D cardiac anisotropy. *ACS Nano* 11, 5646–5659
119. Liu, Y. *et al.* (2016) Tuning the conductivity and inner structure of electrospun fibers to promote cardiomyocyte elongation and synchronous beating. *Mater. Sci. Eng. C* 69, 865–874
120. Qazi, T.H. *et al.* (2015) Biomaterials based strategies for skeletal muscle tissue engineering: existing technologies and future trends. *Biomaterials* 53, 502–521
121. Hoffman, W.Y. *et al.* (2015) Human satellite cell transplantation and regeneration from diverse skeletal muscles. *Stem Cell Reports* 5, 419–434
122. Forcales, S.V. (2015) Potential of adipose-derived stem cells in muscular regenerative therapies. *Front. Aging Neurosci.* 7, 1–12
123. Jo, H. *et al.* (2017) Electrically conductive graphene/polyacrylamide hydrogels produced by mild chemical reduction for enhanced myoblast growth and differentiation. *Acta Biomater.* 48, 100–109
124. Mahmoudifard, M. *et al.* (2016) The different fate of satellite cells on conductive composite electrospun nanofibers with graphene and graphene oxide nanosheets. *Biomed. Mater.* 11, 25006
125. Shima, A. *et al.* (2018) Three-dimensional contractile muscle tissue consisting of human skeletal myocyte cell line. *Exp. Cell Res.* 370, 168–173
126. Raman, R. *et al.* (2017) A modular approach to the design, fabrication, and characterization of muscle-powered biological machines. *Nat. Protoc.* 12, 519–533
127. Kim, T.H. *et al.* (2016) Bio-inspired hybrid carbon nanotube muscles. *Sci. Rep.* 6, 6–13
128. Björninen, M. *et al.* (2017) Electrically stimulated adipose stem cells on polypyrrole-coated scaffolds for smooth muscle tissue engineering. *Ann. Biomed. Eng.* 45, 1015–1026
129. Byambaa, B. *et al.* (2018) Advances in osteobiologic materials for bone substitutes. *J. Tissue Eng. Regen. Med.* 12, 1448–1468

130. Sayyar, S. *et al.* (2016) UV cross-linkable graphene/poly(trimethylene carbonate) composites for 3D printing of electrically conductive scaffolds. *ACS Appl. Mater. Interfaces* 8, 31916–31925
131. He, Y. *et al.* (2017) Synthesis of polypyrrole nanowires with positive effect on MC3T3-E1 cell functions through electrical stimulation. *Mater. Sci. Eng. C* 71, 43–50
132. Paun, I.A. *et al.* (2015) Electrically stimulated osteogenesis on Ti-PPy/PLGA constructs prepared by laser-assisted processes. *Mater. Sci. Eng. C* 55, 61–69
133. Zhang, J. *et al.* (2016) Electrical stimulation of adipose-derived mesenchymal stem cells in conductive scaffolds and the roles of voltage-gated ion channels. *Acta Biomater.* 32, 46–56
134. Zhang, J. *et al.* (2018) Electrical stimulation of adipose-derived mesenchymal stem cells and endothelial cells co-cultured in a conductive scaffold for potential orthopaedic applications. *J. Tissue Eng. Regen. Med.* 12, 878–889
135. Leppik, L. *et al.* (2018) Combining electrical stimulation and tissue engineering to treat large bone defects in a rat model. *Sci. Rep.* 8, 1–14
136. Zhu, S. *et al.* (2017) Time-dependent effect of electrical stimulation on osteogenic differentiation of bone mesenchymal stromal cells cultured on conductive nanofibers. *J. Biomed. Mater. Res. A* 105, 3369–3383
137. Hu, W.-W. *et al.* (2018) The effects of substrate-mediated electrical stimulation on the promotion of osteogenic differentiation and its optimization. *J. Biomed. Mater. Res. B Appl. Biomater.* 107, 1607–1619
138. Ravikumar, K. *et al.* (2017) Synergy of substrate conductivity and intermittent electrical stimulation towards osteogenic differentiation of human mesenchymal stem cells. *Bioelectrochemistry* 116, 52–64
139. Liu, Z. *et al.* (2017) Mediation of cellular osteogenic differentiation through daily stimulation time based on polypyrrole planar electrodes. *Sci. Rep.* 7, 1–10
140. Jamal, D. and de Guzman, R.C. (2017) Silicone substrate with collagen and carbon nanotubes exposed to pulsed current for MSC osteodifferentiation. *Int. J. Biomater.* 2017, 1–9
141. Çakmak, A.S. *et al.* (2016) Synergistic effect of exogeneous and endogeneous electrostimulation on osteogenic differentiation of human mesenchymal stem cells seeded on silk scaffolds. *J. Orthop. Res.* 34, 581–590
142. Oftadeh, M.O. *et al.* (2018) Sequential application of mineralized electroconductive scaffold and electrical stimulation for efficient osteogenesis. *J. Biomed. Mater. Res. A* 106, 1200–1210
143. Alberts, B. *et al.* (2002) Molecular Biology of the Cell, 4th edn (Garland Science)
144. Balint, R. *et al.* (2013) Electrical stimulation: a novel tool for tissue engineering. *Tissue Eng. B Rev.* 19, 48–57
145. Nicholson, R.S. (1965) Theory and application of cyclic voltammetry for measurement of electrode reaction kinetics. *Anal. Chem.* 37, 1351–1355
146. Zhao, W.-S. *et al.* (2019) Mini-Review: Modeling and performance analysis of nanocarbon interconnects. *Appl. Sci.* 9, 2174
147. Das, P. *et al.* (2017) Dual growth factor loaded nonmulberry silk fibroin/carbon nanofiber composite 3D scaffolds for *in vitro* and *in vivo* bone regeneration. *Biomaterials* 136, 67–85